ANL-AFCI-216

Argonne NATIONAL LABORATORY

OSMOSE
An Experimental Program for Improving Neutronic Predictions of Advanced Nuclear Fuels

Topical Report

Nuclear Engineering Division

About Argonne National Laboratory

Argonne is a U.S. Department of Energy laboratory managed by UChicago Argonne, LLC under contract DE-AC02-06CH11357. The Laboratory's main facility is outside Chicago, at 9700 South Cass Avenue, Argonne, Illinois 60439. For information about Argonne, see www.anl.gov.

Availability of This Report

This report is available, at no cost, at http://www.osti.gov/bridge. It is also available on paper to the U.S. Department of Energy and its contractors, for a processing fee, from:

U.S. Department of Energy
Office of Scientific and Technical Information
P.O. Box 62
Oak Ridge, TN 37831-0062
phone (865) 576-8401
fax (865) 576-5728
reports@adonis.osti.gov

ANL-AFCI-216

OSMOSE
An Experimental Program for Improving Neutronic Predictions of Advanced Nuclear Fuels

Topical Report

by

R. T. Klann, G. Aliberti, Z. Zhong, and D. Graczyk
Nuclear Engineering Division, Argonne National Laboratory

A. Lyoussi
Cadarache, Commissariat à l'Energie Atomique, France

2007 Annual Report

OSMOSE
An Experimental Program for Improving Neutronic Predictions of Advanced Nuclear Fuels

2007 Annual Report

Lead US Investigating Organization: Argonne National Laboratory
US Principal Investigator: Raymond T. Klann

Lead Collaborating Investigating Organization: CEA-Cadarache
Lead Collaborating Principal Investigator: Abdallah Lyoussi

Period of Performance: 10/1/06 to 9/30/07

Authors:
Raymond T. Klann
Abdallah Lyoussi
Gerardo Aliberti
Zhaopeng Zhong
Donald Graczyk

Abstract

This report describes the technical results of tasks and activities conducted in FY07 to support the DOE-CEA collaboration on the OSMOSE program. The activities are divided into five high-level tasks: reactor modeling and pre-experiment analysis, sample fabrication and analysis, reactor experiments, data treatment and analysis, and assessment for relevance to high priority advanced reactor programs (such as GNEP and Gen-IV).

Table of Contents

List of Tables

List of Figures

1. Purpose

The OSMOSE program aims at improving neutronic predictions of advanced nuclear fuels through measurements in the MINERVE facility on samples containing the following separated actinides : ^{232}Th, ^{233}U, ^{234}U, ^{235}U, ^{236}U, ^{238}U, ^{237}Np, ^{238}Pu, ^{239}Pu, ^{240}Pu, ^{241}Pu, ^{242}Pu, ^{241}Am, ^{243}Am, ^{244}Cm and ^{245}Cm. The continuation of the DOE/CEA collaboration on the OSMOSE program includes: the participation of DOE in the conduct of the experiments, the development and comparison of analytic tools and models of CEA and DOE based on Monte Carlo and deterministic methods, and the assessment of oscillation measurements for validation of cross-sections pertinent to high priority advanced reactor programs (such as GNEP and NGNP).

The goal of the experimental measurements is to produce a database of reactivity-worth measurements in different neutron spectra for the separated heavy nuclides. This database can then be used as a benchmark for integral reactivity-worth measurements to verify and validate reactor analysis codes and integral cross-section values for the isotopes tested. Based on the reduction of uncertainties in the measurements, the target improvements in integral cross-section parameters are shown in Table 1.

Table 1:

Target Improvements in Nuclear Data from the OSMOSE Program

Actinide	Parameter	Current Uncertainty (at 1σ)	Target Uncertainty (at 1σ)
U233	η_{therm}	± 2500 pcm	± 1500 pcm
	$\eta_{epitherm}$	± 4000 pcm	± 2500 pcm
U234	I_r	± 10 %	± 3 %
	σ_c^{th}	± 2 %	± 1.5 %
U236	I_r	± 5 %	± 3 %
Np237	I_r	± 7 %	± 2 %
	σ_c^{th}	± 3 %	± 1.5 %
Pu238	I_r	± 9 %	± 4 %
	σ_c^{th}	± 2 %	± 1.5 %
Pu239	η_{therm}	± 3000 pcm	± 2000 pcm
	$\eta_{epitherm}$	± 4000 pcm	± 2000 pcm
Pu240	I_r	± 3 %	± 1.5 %
Pu242	I_r	± 4 %	± 2 %
Am241	I_r	± 7 %	± 2 %
	σ_c^{th}	± 3 %	± 1.5 %
Am243	I_r	± 5 %	± 3 %
Cm244	I_r	± 5 %	± 3 %
Cm245	η_{therm}	± 4000 pcm	± 1500 pcm
Th232	I_r	± 4 %	± 2 %

Ir = resonance integral, σ_c^{th} = microscopic capture cross section, η = reproduction factor

2. Project Description

The project includes five high level tasks – reactor modeling and pre-experiment analysis, sample fabrication, reactor experiments, data treatment and analysis, and assessment for relevance to high priority reactor programs. The analytic effort is being performed by ANL and CEA personnel using MCNP and separate suites of reactor analysis codes. In this manner, a cross comparison can be performed on the results to identify potential errors in the cross-section evaluations and the numerical methods and assumptions used within the codes. This will allow the improvement of these codes.

The pre-experiment reactor modeling effort provides detailed foreknowledge for planning the experimental measurements. It also allows detailed models of the different core configurations to be assembled which can be used to support the data treatment and analysis of the experimental results. This modeling effort also provides the opportunity to thoroughly check the data on the reactor configuration including the fuel and structural materials, composition, geometry, and operating conditions.

The measurement program is utilizing the MINERVE reactor, which is a low-power uranium fueled pool reactor. The normal accuracy for measurements of small-worth samples in this reactor is on the order of 1% for relative reactivity worths. Including the uncertainties associated with the composition of the samples (~2% on the analysis) and the uncertainties associated with the calculations (~2% on the model and calibration samples), the total uncertainties for the OSMOSE program are estimated to be approximately 3%. In this reactor, sample reactivity differences of less than one cent have been routinely measured. Accuracies in small-sample reactivity worths this low are only achieved through oscillator techniques. In MINERVE, the so-called auto-rod, or closed-loop, technique is used. The total worth of the auto-rod is about 6 cents, which allows accurate reactivity comparisons.

The experimental technique consists of oscillating characterized samples (containing the nuclide of interest) in the lattices of MINERVE. The reactivity variation of the sample is compensated by a calibrated rotary automatic pilot using cadmium sectors. The experimental precision is better than 1%. Other measurements of spectral indices, such as the conversion ratio of ^{238}U, and radial and axial reaction rate distributions, are also performed in order to fit the neutronic characterization of the studied lattices.

Seven different neutron spectra can be created in the MINERVE facility: UO_2 dissolved in water (representative of over-moderated LWR systems), UO_2 matrix in water (representative of LWRs), mixed oxide fuel matrix, two thermal spectra containing large epithermal components (representative of under-moderated reactors), moderated fast spectrum (representative of fast reactors which have some slowing down due to moderators such as lead-bismuth or sodium), and a very hard spectrum (representative of fast reactors with little moderation from reactor coolant). The different spectra are achieved by changing the lattice within the MINERVE reactor. This configuration leads to a uniform well-behaved system such that the reactor configuration is in the fundamental mode, which allows for simple spatial analysis methods.

The OSMOSE experimental program will produce very accurate sample worth measurements for a series of actinides in various spectra, from very thermalized to very fast. The objective of the

analytical program is to make use of this experimental data to establish deficiencies in the basic nuclear data libraries, identify their origins, and propose paths towards correcting them, in coordination with international nuclear data programs.

A fundamental property of the oscillation experiments performed in the OSMOSE program is that the neutron flux at the sample location has reached the asymptotic fundamental mode of the MINERVE lattice (note that this is the replaceable central part of MINERVE, which establishes the spectrum at the sample location). This property allows for the use of simple spatial analysis methods (e.g. a lattice code with axial buckling representing the leakage) without loss of accuracy. The computational challenge is then reduced to the need for correct representation of cross-sections and for accurate resonance shielding algorithms. Modern codes (commercial lattice codes, Monte Carlo codes, etc.) have such high quality algorithms that cross-comparisons between codes will be used to eliminate potential algorithmic deficiencies. Thus the comparison of calculated to experimental values (C/E) will yield direct information on cross-section weaknesses.

Sensitivity calculations were run using information from the measurements in several spectra, in order to pinpoint the origin of observed discrepancies and propose possible solutions. In addition, the relevance of each spectrum, and combinations of the different spectra, will be determined with respect to representative spectra for advanced reactor concepts under development for advanced reactor programs like GNEP, NGNP, and Gen-IV. This assessment provides a numerical ranking of representativeness for these programs and will allow for planning and prioritization of experimental measurements.

3. Project Organization:

Roles and Responsibilities for activities and tasks associated with the OSMOSE project are as defined in Table 2.

Table 2
Roles and Responsibilities for Each Organization

Task Description	Lead	Support
Task 1: Reactor Modeling	ANL	CEA-Cadarache
Task 2: Sample Fabrication and Analysis	CEA-Valrhô	ANL
Task 3: Experiments and Data Treatment	CEA-Cadarache	ANL
Task 4: Assessment for Advanced Reactor Programs	ANL	CEA-Cadarache

4. Results and Status

The project includes five high level tasks – reactor modeling and pre-experiment analysis, sample fabrication, reactor experiments, data treatment and analysis, and assessment for relevance to high priority reactor programs. Results and progress on each task are reported separately below.

4.1. Reactor Modeling for Pre-Experiment Analysis and Planning

Reactor modeling and analysis for pre-experiment planning was performed for two reactor configurations – the R2-UO2 configuration (representative of an overmoderated thermal spectrum) and the MORGANE-R configuration (representative of a thermal spectrum with a large epithermal component) [1]. These are the next two configurations that are scheduled for experimental measurements in the MINERVE facility in 2008.

4.1.1. Calculational Model

The DRAGON deterministic transport code [2] was used for the reactivity worth calculations. DRAGON is a lattice physics code based on the collision probability method. The two main components of the DRAGON code are a multi-group flux solver module and a one group collision probability (CP) tracking module. The different CP tracking modules perform the same tasks but with different levels of approximation.

The JPM tracking option uses the interface current technique at the level of each homogeneous zone associated with a specific geometry ($J\pm$ method). With this option, one can either build the complete collision probabilities matrix or generate a response matrix both of which can be processed by the general multi-group solver. The last method permits a non-iterative calculation of the one group neutron flux to be carried out using sparse matrix algebra.

The SYBIL tracking option emulates the main flux calculation option available in the APOLLO-1 code, and includes a new version of the EURYDICE-2 code which performs reactor assembly calculations in both rectangular and hexagonal geometries using the interface current method. SYBIL is slightly more accurate than JPM because it performs a complete calculation of the collision probabilities on the whole or a large part of the domain thereby avoiding a large number of interfaces for the angular flux approximation.

The EXCELL tracking option is used to generate the collision probability matrices for the cases having cluster, two dimensional or three dimensional mixed rectangular and cylindrical geometries. A cyclic tracking option is also available for treating specular boundary conditions in two dimensional rectangular geometries. After the collision probability or response matrices associated with a given cell have been generated, the multi-group solution module can be activated. This module uses the power iteration method and requires a number of iteration types. The thermal iterations are carried out by DRAGON so as to rebalance the flux distribution only in cases where neutrons undergo upscattering. The power iterations are performed by DRAGON to solve the fixed source or eigenvalue problem in the cases where a multiplicative medium is analyzed. The effective multiplication factor (k_{eff}) is obtained during the power iterations. A search for the critical buckling may be superimposed upon the power iterations to force the multiplication factor to take on a fixed value.

The calculation model for the R1-MOX configuration consisted of a two-dimensional (11×11) multi-cell mini-lattice corresponding to the experimental zone of the MINERVE reactor. Due to the symmetry of geometry, actually only $1/8^{th}$ model was introduced. The model for the R1-MOX configuration is shown in Figure 1. The sample pin is located in the center, surrounded

with MOX pins. The model for R2-UO2 is shown in Figure 2. It is similar to the R1-UO2 model [3], the only difference is that 8 water pins surround the sample pin.

For the MORGANE/R configuration, the hexagonal geometry capability of DRAGON was utilized, and the whole domain was composed of hexagonal cells. Due to the geometry limit of DRAGON, an approximate $1/12^{th}$ model was developed for MORGANE/R, which is shown in Figure 3. Because the size of the the guide tube surrounding the sample pin cell is larger than the hexagonal lattice used for the pin cells of normal MOX fuel, only the fuel and clad of the sample pin was included and the guide tube was neglected. To study the spectral change caused by this approximation, an MCNP calculation was performed for the MORGANE/R configuration loaded with the natural UO2 sample, the comparison of the spectra for the case with the guide tube and without the guide tube is shown in Figure 4. It can be seen that removing the guide tube surrounding the sample pin causes very little change in the spectrum.

ENDF/B-VI and JEFF3.1 based WIMS-D4 format 172-group neutron libraries were used for the DRAGON calculations. The surface net current coupling option, SYBLIT, was also used for the calculations.

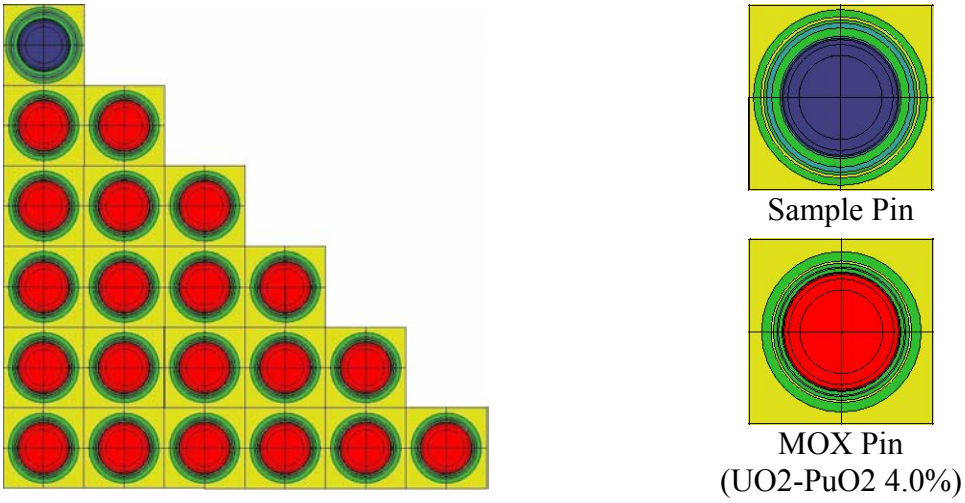

Figure 1: DRAGON Calculation Model for the R1-MOX Configuration

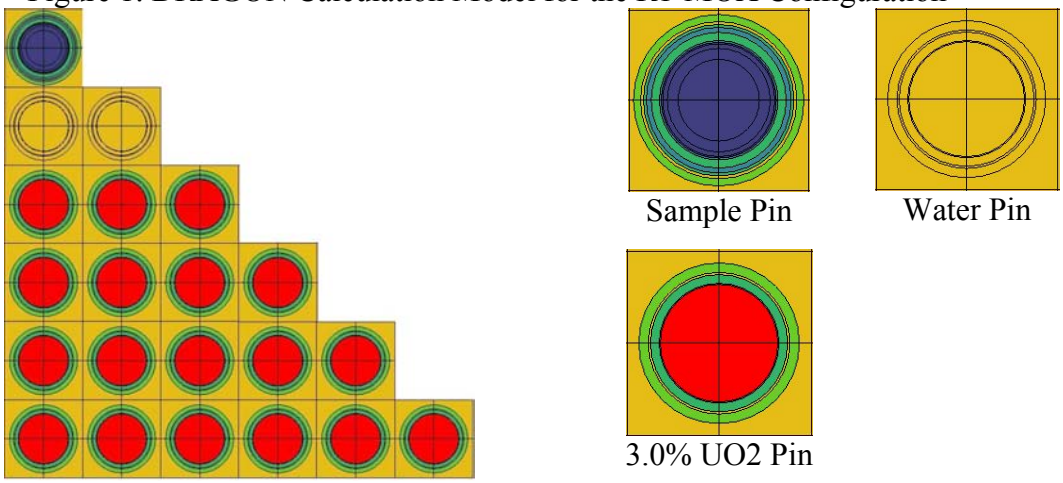

Figure 2: DRAGON Calculation Model for the R2-UO2 Configuration

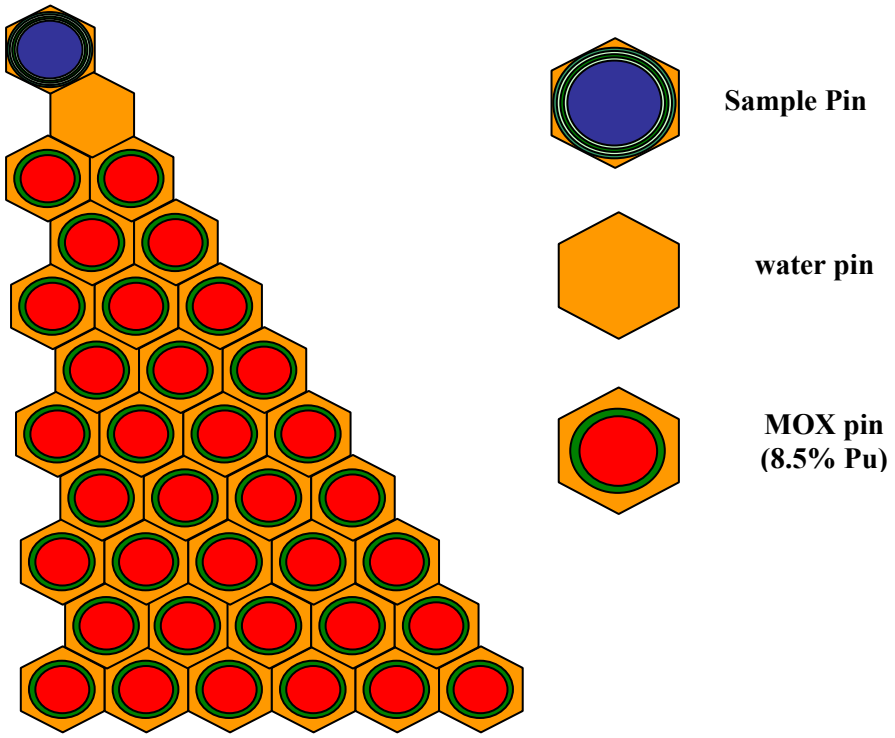

Figure 3: DRAGON Calculation Model for the MORGANE/R Configuration

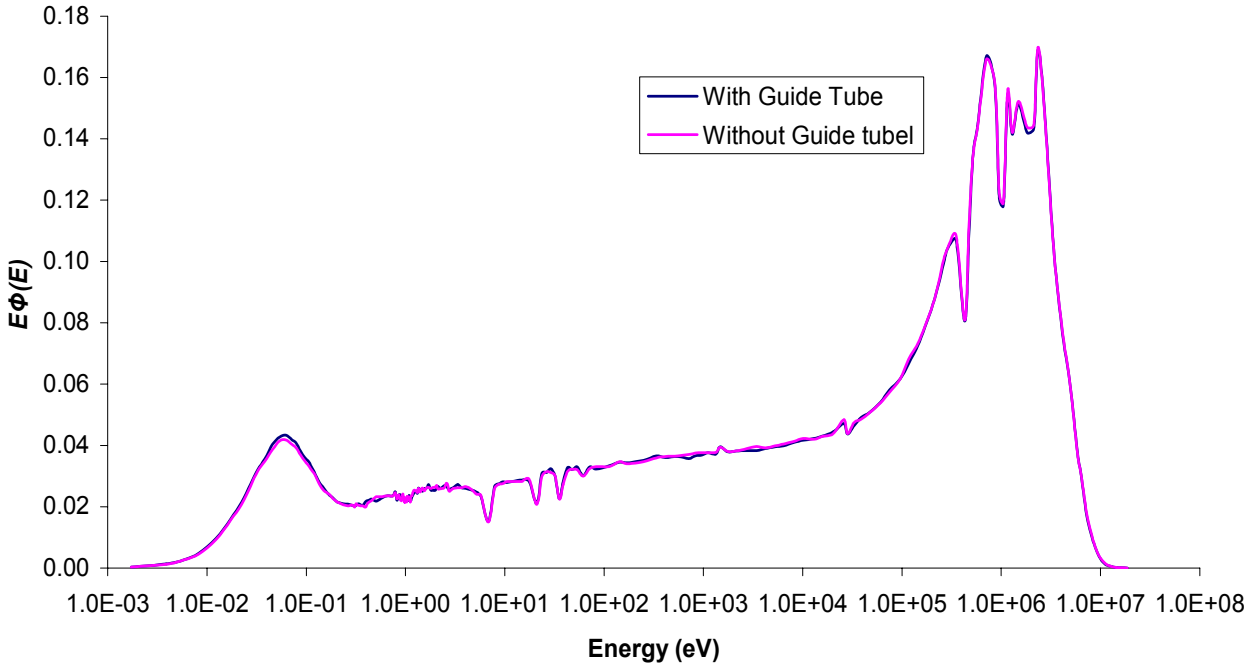

Figure 4: Spectral Effect Caused by the Guide Tube

4.1.2. Spectral Comparison

A series of calculations were performed to calculate the spectra of OSMOSE configurations using the DRAGON code with the ENDF6-172 group library. The comparison of the spectra for different OSMOSE configurations are shown in Figure 5, and are consistent with expected results. The R2-UO2 configuration displays the largest thermal flux, whereas, the MORGANE/R configuration, displays the smallest thermal fraction. This is expected since the R2-UO2 configuration represents over-moderation and the MORGANE/R configuration is under-moderated.

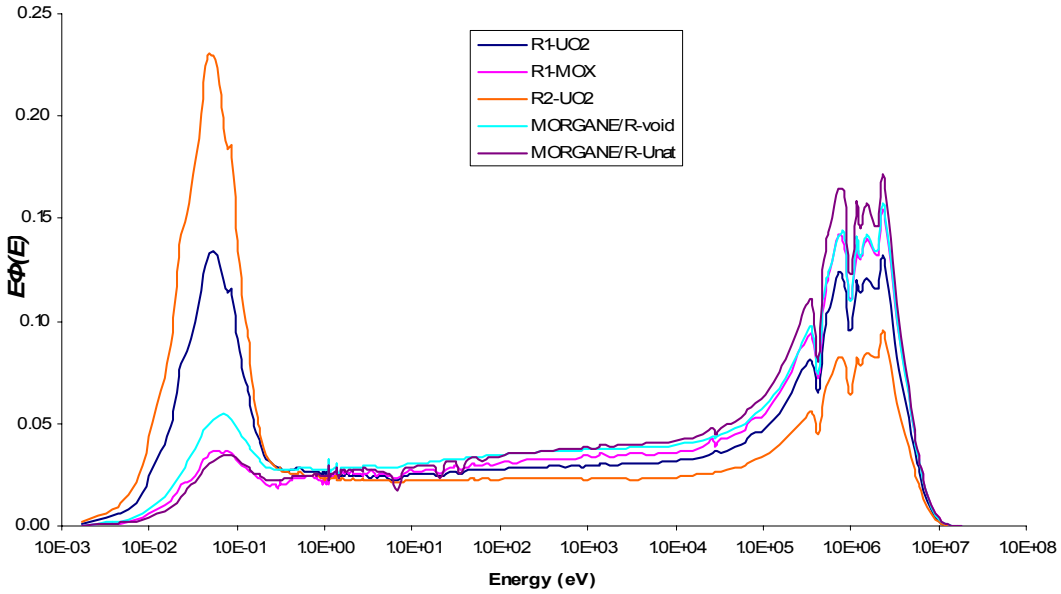

Figure 5: Comparison of Spectra with Different OSMOSE Configurations

4.1.3. Reactivity-Worth Comparison

DRAGON calculations were also performed to obtain reactivity-worth estimates of the OSMOSE samples in the R2-UO2, R1-MOX and MORGANE/R configurations. The results are shown in Tables 3, 4, 5 and Figures 6, 7, and 8.

The reactivity-worth estimate for a sample is not directly computed. The reactivity-worth of a sample is computed by subtracting the calculated reactivity of the configuration with the natural uranium sample in the experimental region from the calculated reactivity of the configuration with the sample in place. So for a given configuration, the reactivity-worth of the samples is referenced to the natural uranium sample which has a reactivity-worth of zero. If a sample has a negative reactivity-worth then it has a higher absorption rate than natural uranium. A positive reactivity-worth implies that a sample has a lower absorption rate or that the sample has a higher fission rate than natural uranium.

In the DRAGON calculations, the effective multiplication factor (k*eff*) is calculated with a superimposed critical buckling. For the calculation of the R2-UO2, MORGANNE/R and R1-

MOX configurations, the critical buckling is searched to force the k_{eff} to be 1.0 for the lattice loaded with the H5 oscillation sample (2.0 % enrichment of U235).

From the results, it is observed that the OSMOSE samples in the R2-UO2 configuration have the largest relative reactivity-worth, and in the MORGANE/R configuration the samples have the smallest reactivity-worth. This trend is as expected and is due to the neutron energy spectrum in the sample location. As the spectrum becomes harder, i.e. the thermal fraction decreases and the fast fraction increases, the number of neutron interactions in the sample decreases due to the lower thermal neutron flux. The relative reactivity-worth is subsequently reduced because it is a measure of the reaction rates (fission and absorption) in the sample.

Table 3:
Reactivity-Worth of the OSMOSE Samples in the R2-UO2 Configuration

Samples	ENDF6 172-group library		JEFF3.1 172-group library	
	k-eff	reactivity worth (pcm)	k-eff	Reactivity worth (pcm)
AM41_1	0.99607	-78.3	0.99595	-86.8
AM41_2	0.99444	-243.0	0.99416	-267.7
AM43	0.99642	-42.9	0.99640	-42.0
NP37_1	0.99643	-41.6	0.99643	-38.6
NP37_2	0.99448	-238.3	0.99463	-220.4
PU38	0.99469	-217.5	0.99475	-207.7
PU39	1.00030	346.9	1.00026	345.4
PU40	0.99533	-153.0	0.99533	-149.9
PU41	0.99806	122.1	0.99799	118.1
PU42	0.99638	-47.1	0.99636	-46.0
U233	0.99957	273.4	0.99952	272.1
U234	0.99619	-65.6	0.99620	-61.7
Unat	0.99685	0.0	0.99681	0.0
URE	1.00165	480.7	1.00160	479.0
U-TH232	0.99651	-33.9	0.99647	-34.3
TH232	0.99327	-361.1	0.99317	-367.8

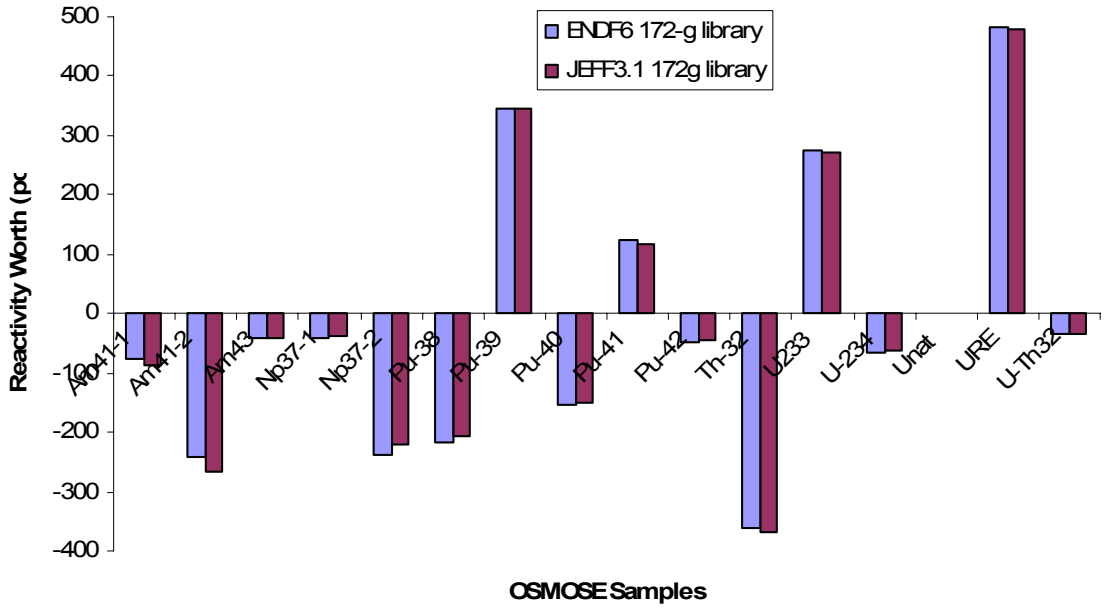

Figure 6: Reactivity-Worth of the OSMOSE Samples in the R2-UO2 Configuration

Table 4:
Reactivity-Worth of the OSMOSE samples in the MORGANE/R Configuration

Samples	ENDF6 172-group Library		JEFF3.1 172-group library	
	k-eff	reactivity worth (pcm)	k-eff	reactivity worth (pcm)
AM41_1	0.99917	-22.2	0.99912	-25.3
AM41_2	0.99872	-68.1	0.99861	-76.8
AM43	0.99921	-18.7	0.99919	-18.5
NP37_1	0.99927	-13.0	0.99925	-12.5
NP37_2	0.99866	-73.5	0.99867	-70.7
PU38	0.99900	-40.8	0.99899	-39.1
PU39	0.99736	34.0	0.99972	34.0
PU40	0.99886	-53.4	0.99885	-52.4
PU41	0.99958	18.6	0.99955	17.7
PU42	0.99919	-20.2	0.99918	-19.8
U233	0.99992	51.9	0.99989	51.6
U234	0.99921	-18.7	0.99920	-17.4
Unat	0.99940	0.0	0.99938	0.0
URE	0.99997	57.0	0.99994	56.7
U-TH232	0.99928	-11.2	0.99926	-11.4
TH232	0.99897	-42.6	0.99893	-44.6

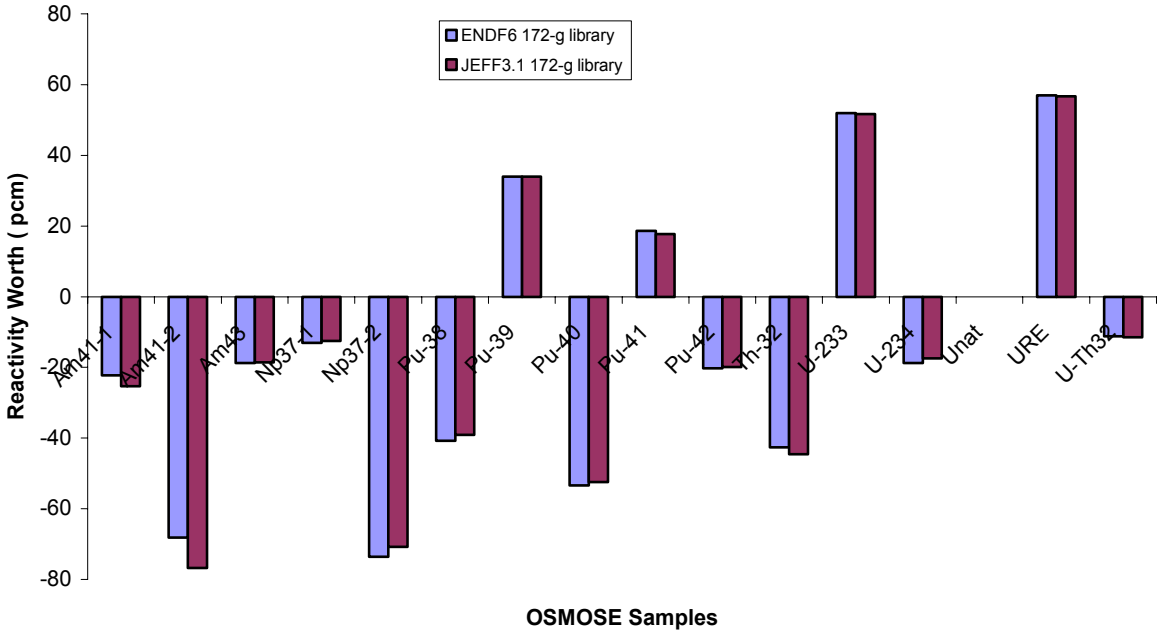

Figure 7: Reactivity-Worth of the OSMOSE Samples in the MORGANE/R Configuration

Table 5: Reactivity-Worth of the OSMOSE Samples in the R1-MOX Configuration		
Samples	JEFF3.1 172-group library	
	k-eff	Reactivity worth (pcm)
AM41_1	0.99920	-33.84
AM41_2	0.99851	-102.70
AM43	0.99927	-27.43
NP37_1	0.99936	-18.42
NP37_2	0.99851	-103.30
PU38	0.99908	-45.66
PU39	1.00020	65.72
PU40	0.99894	-60.19
PU41	0.99982	28.02
PU42	0.99925	-29.14
U233	1.00042	87.60
U234	0.99929	-24.73
Unat	0.99954	0.00
URE	1.00051	96.70
U-TH232	0.99937	-17.22
TH232	0.99878	-122.15

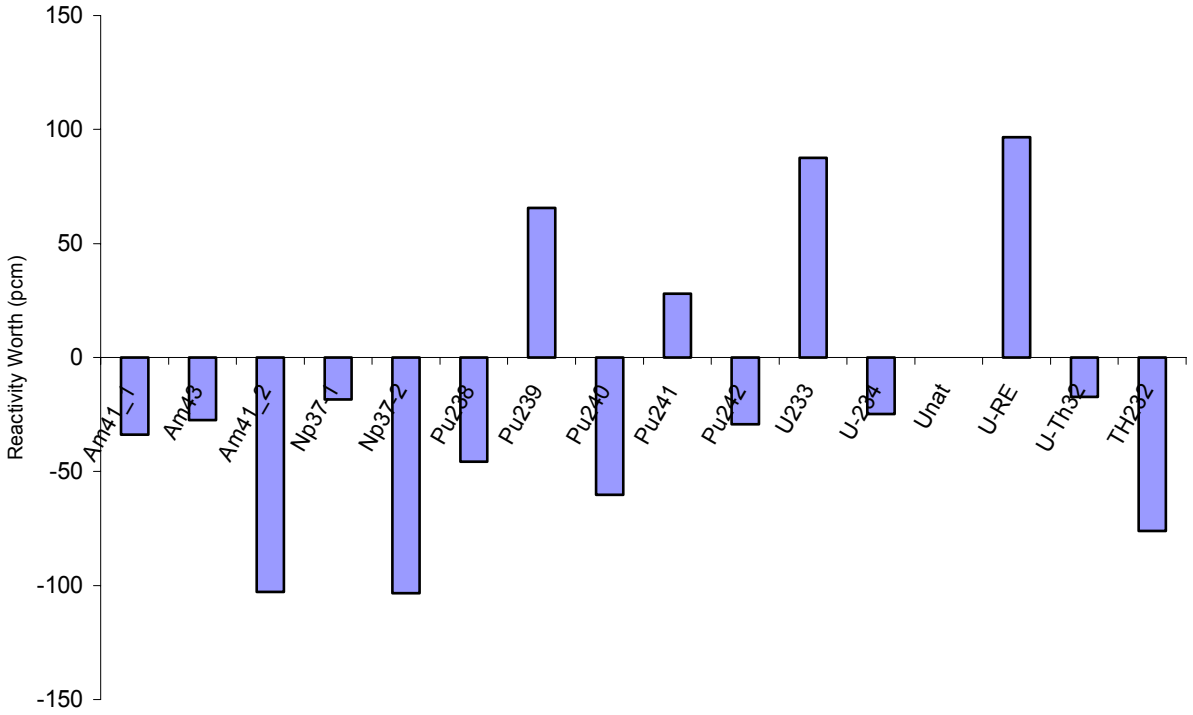

Figure 8: Reactivity-Worth of the OSMOSE Samples in the R1-MOX Configuration

4.1.4. Validation and C/E Comparison

To validate the calculations, a comparison was performed between experimental measurements and calculated results for the R1-MOX configuration loaded with calibration and oscillation samples. The calculation model is based on the DRAGON lattice physics code using the IAEA 172-group JEFF3.1 cross-section library.

The process for comparison can be summarized as follows:

1) Perform measurements to obtain the experimental signal for calibration samples with well-known cross sections and OSMOSE samples

2) Calculate the k_{eff} for the calibration samples with well known cross sections using the validated model and compare it to the experimental signal obtained from step 1 to generate the calibration curve (linear function).

3) Calculate the k_{eff} for the OSMOSE samples using the validated model and compare it to the calibration curve obtained from step 2. If a significant difference is found, it is generally due to the cross section.

For the R1-MOX configuration, the comparison of calculated results and experimental data has been performed using preliminary experimental results. Table 6 shows the calculated k_{eff} of the B-10 and U-235 calibration samples, as well as the experimental signal (in pilot units).

Table 6: Calculated Eigenvalue and Experimental Signals of the Calibration Samples				
Sample	Enrichment of U235 (wt. %)	Boron Density (ppm)	*k-eff*	Experimental Signal
H1	0.25	0	0.99935	2,834
H2	0.50	0	0.99945	8,711
H3	0.71	0	0.99953	16,300
H4	1.00	0	0.99964	24,001
H5	2.00	0	1.00001	53,997
H6	3.00	0	1.00034	80,958
H7	4.00	0	1.00064	102,595
H8	5.00	0	1.00091	123,183
1B0150	0.25	150	0.99899	-26,381
2B0333	0.53	333	0.99872	-49,717

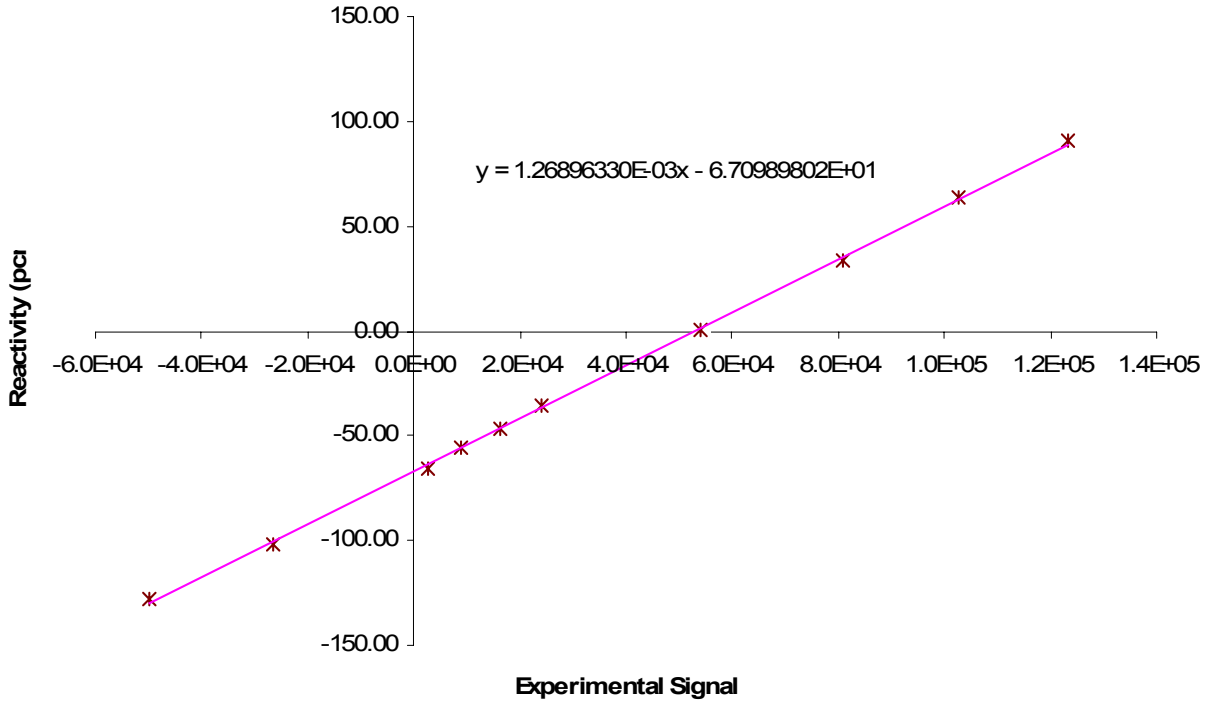

Figure 9: Calibration Curve for R1-MOX Configuration

Figure 9 is the calibration curve, which shows the relation between the experimental signal (in pilot units) of the B-10 and U-235 calibration samples and the calculated eigenvalues (given by the DRAGON 2D model). It has been observed that for the calibration samples (the composition is UO2 fuel with different enrichments in ^{235}U and with a range of boron concentrations), the calculated reactivity worth is almost perfectly linear with the value of experimental signal, as shown in Figure 9, with a root mean square less than 0.02. This shows that the data for the major actinides, ^{235}U and ^{238}U, in the ANL ENDF/B-VI library is sufficiently accurate over this energy region.

Using the function between k_{eff} and experimental signal determined in Figure 9, as well as the experimental signals for the OSMOSE samples in the R1-MOX configuration, the "experimental" reactivity-worth and calculated reactivity-worth of the OSMOSE samples can be predicted. The comparison to the calculated results is shown in Table 7. It can be observed that the agreement between the calculated and experimental results is excellent for some of the samples and marginally acceptable for most of the other samples. However, for the Pu242 sample there is a large discrepancy between the calculated and experimental values. The results are being reviewed. These comparisons are only preliminary, because the experimental signals have not been validated yet and the sample analysis results are still pending. Each of these factors could easily explain the discrepancy in the results for the Pu242 sample as well as others.

Table 7:
C/E Comparison of the OSMOSE Samples in the R1-MOX Configuration

OSMOSE Samples	Calculated Reactivity-Worth (pcm)	Experimental Reactivity-Worth (pcm)	(C-E)/E in %
Np237-1	-18.42	-17.33	6.31
Np237-2	-103.30	-97.57	5.88
Pu239	65.72	64.46	1.95
Pu242	-29.14	-24.20	20.39
U234	-24.73	-22.93	7.84
U-Th232	-17.22	-17.23	-0.05
U-RE	96.70	97.98	-1.32
Am41-1	-33.84	-34.16	-0.93
Am41-2	-102.70	-96.31	6.63

4.2. Sample Fabrication and Analysis

The sample fabrication activities are being performed by CEA-Valrho in Marcoule. To help reduce uncertainties on the experimental measurements, ANL is providing post-fabrication destructive analysis of OSMOSE sample pellets for isotopic composition and impurities. These additional sample characterizations will allow a reduction in the uncertainty on the sample compositions (primarily for the minor actinides) and will be reflected in a reduction in the total uncertainty on the experimental measurements and data treatment.

4.2.1. Sample Fabrication and Analysis at CEA-Valrho

In the framework of the OSMOSE program 21 oxide samples containing separated actinides (^{232}Th, ^{233}U, ^{234}U, ^{235}U, ^{236}U, ^{238}U, ^{237}Np, ^{238}Pu, ^{239}Pu, ^{240}Pu, ^{241}Pu, ^{242}Pu, ^{241}Am, ^{243}Am and ^{244}Cm, $^{244+245}$Cm) are to be fabricated. The samples consist of assembled sintered or green fuel pellets containing the isotopes of interest contained in a double zircaloy cladding.

Specifications for the samples include pellet morphology and dimension, pellet density, homogeneity of the distribution of the actinides inside the UO_2 and U_3O_8 matrix, minimization of

chemical pollution or cross-contamination of the samples during the fabrication, and welding and leakage control.

The sample fabrication tasks include pellet fabrication, cladding and welding, shipment of the samples, and chemical analysis. Progress in each area is described separately.

4.2.1.1. Pellet Fabrication

OSMOSE sample pellet fabrication and analysis (isotopic composition vs mass ratio) was completed for the first two sample batches (except for ThO2) in the first quarter of 2006 and the second quarter of 2007 respectively.

The last set of pellets is composed of five samples: UO_2 + $^{233}UO_2$; UO_2 + $^{243}AmO_2$; U_3O_8 + $^{244}CmO_2$; U_3O_8 + $^{244+245}CmO_2$ and finally the U_3O_8 reference. The OSMOSE furnace and the uniaxial three-part die were used during the fabrication of the third set of samples. For the samples containing Cm, it was decided not to sinter the pellets with curium isotopes because of the lack of radioprotection of the OSMOSE furnace. As a consequence, a new press was installed in a hot cell of the ATALANTE C10 line which is suitable for the fabrication and the study of high neutron activity compounds.

The green pellets for two samples (^{244}Cm and $^{244+245}Cm$ doped compound) and a set of uranium sesquioxide for calibration were fabricated. Table 8 summarizes the main characteristics of the last batch of samples. For the sintered pellets, although the mean density of the samples appears a little low, good agreement with the specifications was obtained especially on the diameter. For the Cm green pellets, the diameter obtained after pressing is very close to the target value.

Table 8
Metrology of the Third Set of Pellets

Sample	Target composition (g)	Mean density (%T.D)	Mean ∅ (mm)	D ∅ (mm)
UO_2-^{233}U	0.474	93.7	8.10	0.04
UO_2-^{243}Am	0.608	92.7	8.15	0.02
U_3O_8-^{244}Cm	1.557	59.7*	8.15	<0.10
U_3O_8-$^{244+245}Cm$	0.886	59.0*	8.15	<0.10
U_3O_8 reference		58.3*	8.13	<0.10
Specification		95.0	8.00<∅<8.20	<0.10

* no specification on the density

4.2.1.2. Cladding and Welding

The same procedure that was followed for the first two sample batches was carried out for the cladding and the welding of the batch 3 samples. However, the process was performed in glove boxes (^{233}U) and a hot cell (^{243}Am, ^{244}Cm and $^{244+245}Cm$) due to the radioactivity of the actinide material. In addition, the inner clad of the samples assembled in cell C10 was decontaminated. The welding step included the fabrication of two reference samples and the four OSMOSE samples. After welding of the inner and outer cladding, a leak test was performed. In addition, x-ray and metallographic inspections of the welds were performed on the reference samples.

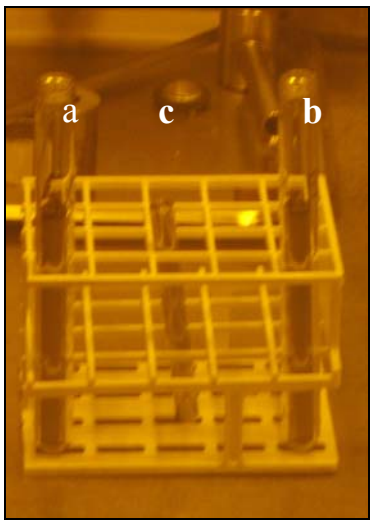

Figure 10: Pins Containing Curium Sample (a, b) and Reference Pin (c)

The curium sample pins are shown in Figure 10.

4.2.1.3. Chemical Analysis

Chemical analysis of the first two batches of samples was completed, however, a final report has not been issued pending the results of the confirmatory chemical analysis being performed by ANL. Analysis of the third batch of samples is ongoing.

Concerning the chemical analysis of the $Th0_2$ samples, some technical difficulties occurred which were connected to the refractory aspect of the components. However this analysis is considered less crucial than the other analyses. Nevertheless, a chemical analysis and assay of another ThO_2 pellet will be performed during the first quarter of 2008.

For the ^{243}Am sample, chemical analysis led to an isotopic composition that was in accordance with the expected values (^{243}Am abundance ratio equal to 99.885 %), however, the obtained content is 15% under the expected value.

Due to a small available quantity of the isotope ^{243}Am, it would not be possible to perform confirmatory chemical analysis if two samples were fabricated in accordance with the objective of the OSMOSE program. In view of this and to obtain acceptable statistical uncertainties on MINERVE oscillation measurements, it was decided to fabricate only one ^{243}Am sample and to perform additional chemical analysis assays.

If the analysis results confirm the initial content with the same discrepancy (15%), the ^{243}Am samples will not be oscillated again. Otherwise, if plutonium impurities are found, which could affect oscillation measurements, the oscillation measurements will be repeated. Chemical analysis of Pu content and the isotopic abundance will be performed on the pellets.

Analysis of the curium samples are expected during the first quarter of 2008.

4.2.2. Chemical Analysis of OSMOSE Pellet Samples at ANL

To help reduce uncertainties associated with the experimental results, ANL is providing post-fabrication destructive analysis of selected OSMOSE sample pellets for isotopic composition and impurities. The ANL sample-analysis activity involves providing corroborative compositional data for one pellet composed of isotopically natural UO_2, and eight pellets composed of the natural uranium matrix doped with specific minor-actinide isotopes [U-234, Th-232, Pu-240, Pu-242, Np-237 (2 levels) and Am-241 (2 levels)].

For the natural uranium pellet, ANL is determining the uranium assay, the uranium isotopic composition, and the concentrations of "absorber" and "banal" impurities. For the actinide-doped pellets, ANL is to measure "as precisely as possible" the mass fraction of the mixed actinide. Where practical, ANL will also determine the isotopic composition of the added actinide.

After a shipping delay while authorizations were pending from Safety Authorities in France, the OSMOSE sample pellets were delivered to ANL in December 2006 and the shipping container was returned to CEA.

ANL's analysis of the natural uranium pellet to determine the uranium mass fraction, uranium isotopic composition, and select impurity elements has been completed. Measurements with the Th-232 and U-234 doped pellets have also been completed. The Pu-240 and Pu-242 doped pellets have been processed and prepared samples are in hand for mass spectrometric analysis to determine (1) the plutonium isotopic composition and mass fraction (by isotope dilution), and (2) the uranium mass fraction, in each pellet. Transfer of these samples from the radioactive materials laboratory to the mass spectrometry laboratory was impeded by an unanticipated, early-July suspension of operations in the nuclear facility where the radioactive materials laboratory is located. All programmatic operations in the facility were halted pending resolution of concerns raised during a DOE assessment. Although delayed, transfer of the plutonium-doped pellet samples to the mass spectrometry laboratory was ultimately accommodated and results for these pellets are anticipated in October. Processing of the Np-doped and Am-doped pellets could not be initiated pending permission to resume activities in the facility. As of September 21, the schedule for resumption of activities in the facility has not been established. This situation has significant implications for the schedule of completing the sample analysis at ANL. The current expectation is that analysis of the Np-doped and Am-doped pellets will be completed by December 31, 2007.

Preliminary results from the samples completed to date are provided in the following sections. It is noted that the data presented here have not been finalized and are subject to revision upon review and verification.

4.2.2.1. Natural Uranium Pellet (Pellet No. MFUO2142)

The pellet containing the undoped-natural-uranium matrix (Pellet No.MFUO2142) was the first to be processed at Argonne. The pellet mass measured at Argonne (3.96367 g) agreed well with the mass provided by CEA (3.963 g). The entire pellet was dissolved in dilute nitric acid with a

trace of hydrofluoric acid to ensure dissolution of impurities. Mass aliquots of the dissolver stock solution were taken for measurement of impurities, uranium isotopics, and uranium assay.

The isotopic composition of uranium in the MFUO2142 pellet was measured by thermal ionization mass spectrometry (TIMS). Instrument bias corrections were determined using NBS SRM U-500 isotopic reference material. Two analyses were carried out with the TIMS; data are summarized in Table 9. The isotopic composition is consistent with the composition of "natural" uranium, except that a trace of U-236 (0.0008 ± 0.0005 percent of U) might be present.

Table 9:
Isotopic Composition of Uranium in Pellet MFUO2142

		U-233	U-234	U-235	U-236	U-238
Atom % Abundance	Run 1:	<0.0005	0.0053	0.7210	0.0008	99.2728
	Run 2:	<0.0005	0.0054	0.7197	0.0007	99.2743
	Average:	<0.0005	0.0053	0.7203	0.0008	99.2736
		± 0.0005	± 0.0005	± 0.0020	± 0.0005	± 0.0020
Mass % Abundance	Run 1:	<0.0005	0.0052	0.7120	0.0008	99.2820
	Run 2:	<0.0005	0.0053	0.7106	0.0007	99.2834
	Average:	<0.0005	0.0053	0.7113	0.0008	99.2827
		± 0.0005	± 0.0005	± 0.0020	± 0.0005	± 0.0020

The mass fraction of uranium in the MFUO2142 pellet was measured in two ways. The first measurement was performed by converting uranyl nitrate salt from three mass aliquots of the pellet solution to U_3O_8, weighing the U_3O_8 product, and converting to equivalent U. [4] The second measurement was carried out using the isotope dilution technique, with three mass aliquots of the pellet solution added to U-235 spikes containing accurately known quantities of NBS SRM 993 U-235 assay standard. Results of the assays are listed in Table 10. Agreement within and between methods was satisfactory. The best estimate of uranium content of pellet MFUO2142 from these data is 88.11 ± 0.13% by mass. This value is comparable to the theoretical uranium mass fraction in UO_2, 88.15 mass %.

Table 10:
Results of Uranium Assays for Pellet MFUO2142

	Uranium Content, mass % (g U per 100 g pellet)	
Replicate	Gravimetric Assay Results	Isotope Dilution Results
1	88.154	88.082
2	88.209	88.150
3	88.210	87.881
Average:	88.191	88.038
Standard Deviation:	0.032	0.140
RSD, %:	0.036	0.159
Grand Average:	88.11 ± 0.13	

Impurity elements in the natural uranium oxide pellet were measured by ICP-MS and ICP-OES after removing uranium with Eichrom U-TEVA resin. Recovery of each impurity through the separation process was evaluated by processing two portions of a solution of the requested elements and by spiking two portions of the pellet solution with the requested-elements solution prior to separating the uranium. Table 11 lists the elements that were analyzed for in the natural uranium pellet, average recoveries obtained with the spiked blank and spiked sample portions, and results for elements recovered at satisfactory levels. Low recoveries were obtained with Ag, Ta, Th, and Zr. The low silver recovery is probably due to chemical matrix effects. The other elements are typically retained with uranium on the U-TEVA resin, which is specific for uranyl ion and tetravalent cations.

The impurities data indicate a presence of two absorber impurities at levels above detection limits: Li at 0.44 ± 0.22 μg/g U and Gd at 0.94 ± 0.20 μg/g U. This gadolinium concentration corresponds to a concentration of Gd-157 of 0.14 ± 0.03 μg/g U. Among the banal impurities, Al, Fe, and W are notable with concentrations at or above 10 μg/g U.

4.2.2.2. Th-232 Doped Pellet (Pellet MFUTH318)

The isotopic composition of uranium in the MFUTH318 pellet was not measured but was taken to be identical with the uranium in the natural uranium pellet as given in Table 9.

The mass fraction of uranium in the MFUTH318 pellet was measured by isotope dilution with three mass aliquots of the pellet solution added to U-235 spikes containing accurately known quantities of NBS SRM 993 U-235 assay standard. Uranium and thorium in the spiked samples were separated using HCl anion exchange with Dowex AG-1x8 resin. Results of the assays are listed in Table 12. The best estimate of uranium content of pellet MFUTH318 from these data is 83.71 ± 0.15 % by mass. This value is comparable to the uranium mass fraction calculated from the uranium and pellet masses (3.441 and 4.104g, resp.) provided by CEA in the pellet description, which correspond to 83.85 mass % U in the pellet.

Thorium fractions for isotopic analysis and isotope dilution assay measurements on the thorium-232 doped pellet (MFUTH318) were analyzed by TIMS. The isotopic analysis indicated that the thorium dopant is very nearly 100% Th-232 (Th-230 is less than 0.05 atom % relative to total thorium in the pellet). This finding is consistent with the CEA pellet description that lists the thorium composition as 99.9% Th-232).

The mass fraction of thorium in the MFUTH318 pellet was measured with three mass aliquots of the pellet solution added to spikes containing accurately known quantities of a Th-230 spike which was standardized some years ago in Argonne's laboratory by comparison with a high-purity ThO_2 reagent. Thorium in the spiked samples was separated using HCl anion exchange with Dowex AG-1x8 resin. Results of the assays are listed in Table 13.

The best estimate of thorium content in pellet MFUTH318 from these data is 4.167 ± 0.013% by mass. This value compares very favorably with the thorium mass fraction calculated from the thorium and pellet masses (0.171 and 4.104g, resp.) provided by CEA in the pellet description, which correspond to 4.167 mass % Th in the pellet. Uncertainty in the thorium assay results includes contributions from the spike standardization as well as an allowance for inaccuracy in

corrections that were applied for instrument bias in the TIMS measurements. Because no reference material is available with a certified thorium isotopic composition, the needed bias correction was estimated from the bias associated with uranium isotopes in the TIMS.

Table 11:
Results of Impurity Measurements for Pellet MFUO2142

	Element	Recovery with Blank Spike, %	Recovery with Spiked Sample, %	Result from Subsample A, µg/gU	Result from Subsample B, µg/gU	Average Result, µg/gU
Absorber Impurities	B	92.3	90.5	< 0.46	< 0.49	< 0.5
	Cd	101.8	100.5	< 0.02	< 0.02	< 0.02
	Li	73.1	79.9	0.60	0.27	0.44
	Gd	103.4	104.0	1.04	0.83	0.94
	Sm	100.2	100.8	< 0.02	< 0.02	< 0.02
	Eu	103.4	101.5	< 0.02	< 0.02	< 0.02
	Dy	102.2	101.4	< 0.02	< 0.02	< 0.02
Banal Impurities	Ag	27.6	12.8	NR	NR	NR
	Al	96.0	NC	8.1	14.9	11.5
	Bi	99.8	98.9	< 0.02	< 0.02	< 0.02
	Ca	79.1	NC	1.9	22.0	12.0
	Co	100.5	101.7	0.12	0.05	0.09
	Cr	100.2	100.1	2.2	2.4	2.3
	Cu	95.1	104.1	2.1	1.3	1.7
	Fe	98.6	NC	18.6	18.3	18.5
	In	103.2	101.9	< 0.02	< 0.02	< 0.02
	Mg	104.6	84.7	3.3	6.1	4.7
	Mn	100.9	101.0	0.19	0.11	0.15
	Mo	102.1	99.4	0.28	0.21	0.25
	Ni	97.1	NC	8.9	2.5	5.7
	Pb	107.8	100.8	0.51	0.43	0.47
	Si	64.4	53.7	3.8	2.7	3.3
	Sn	98.6	60.9	0.27	0.11	0.19
	Ta	4.5	1.3	NR	NR	NR
	Ti	101.6	79.0	4.5	4.6	4.6
	Th	0.0	0.0	NR	NR	NR
	V	101.8	101.6	0.14	0.15	0.15
	W	81.0	NC	19.2	22.3	20.8
	Zn	94.0	79.1	2.6	2.2	2.4
	Zr	3.7	1.1	NR	NR	NR
	Ba	Not Spiked	Not Spiked	< 0.5	< 0.5	< 0.5
	K	Not Spiked	Not Spiked	# 10	# 10	# 10
	Na	Not Spiked	Not Spiked	< 10	< 10	< 10
	Sr	Not Spiked	Not Spiked	0.03	0.05	0.04

NR = Not Reported due to low recovery in separations
NC = Not calculated; spike recovery not calculated because element present in sample

Table 12: Results of Uranium Assays for Pellet MFTH318	
	Uranium Content, mass % (g U per 100 g pellet)
Replicate	Isotope Dilution Results
1	83.740
2	83.577
3	83.814
Average:	83.710 ± 0.15
Standard Deviation:	0.121
RSD, %:	0.145

Table 13: Results of Thorium Assays for Pellet MFTH318	
	Th Content, mass % (g Th per 100 g pellet)
Replicate	Isotope Dilution Results
1	4.166
2	4.168
3	4.167
Average:	4.167 ± 0.013*
Standard Deviation:	0.0014
RSD, %:	0.034

* Uncertainty includes contributions from spike characterization and instrument bias corrections.

4.2.2.3. U-234 Doped Pellet (Pellet MFUU4005):

Because the doping actinide in the U-234 doped pellet is the same element as the matrix actinide (i.e., both uranium), the doping and matrix actinide could not be determined separately from one another. In addition, because the requested assay for U-234 was desired as the ratio of U-234 to total U in the pellet, only isotopic analysis of the pellet uranium was carried out. Two measurements of the uranium isotopic composition were made. Results are shown in Table 14.

Table 14: Isotopic Composition of Uranium in Pellet MFUU4005						
		U-233	U-234	U-235	U-236	U-238
Atom % Abundance	Run 1:	<0.0005	0.7289	0.7157	0.0004	98.5550
	Run 2:	<0.0005	0.7284	0.7157	0.0007	98.5551
	Average:	<0.0005	0.7287	0.7157	0.0006	98.5551
		± 0.0005	± 0.0020	± 0.0020	± 0.0005	± 0.0028
Mass % Abundance	Run 1:	<0.0005	0.7167	0.7068	0.0004	98.5760
	Run 2:	<0.0005	0.7163	0.7068	0.0007	98.5761
	Average:	<0.0005	0.7165	0.7068	0.0006	98.5761
		± 0.0005	± 0.0020	± 0.0020	± 0.0005	± 0.0028

To estimate the ratio of the U-234 doping actinide to natural uranium in the pellet, one needs to know the isotopic composition of the dopant. A calculation was carried out using the dopant isotopic composition provided by CEA, since this isotopic information could not be reliably deduced from Argonne data alone. The result of the calculation was that the mass ratio of U-234 dopant to natural uranium in the pellet is 0.00717 g/g. This value is not out of line with the description provided by CEA, which indicates a ratio (g dopant/gU) of 0.025/3.435 = 0.00728.

4.3. Experiments and Data Treatment

The schedule for conduct of OSMOSE measurements in the MINERVE facility is dictated by commitments for facility operations for several programs at CEA-Cadarache. The R1-MOX configuration was previously loaded in MINERVE in July 2006. Calibration samples were oscillated from September 2006 to January 2007. The first and second batches of OSMOSE samples were then oscillated in the R1-MOX configuration from January 2007 to March 2007. The third batch of OSMOSE sample will be oscillated in MINERVE by December 2007.

Due to the thermal power of the Curium sample material, it was decided to create the OSMOSE samples using a U_3O_8 matrix instead of UO_2 to avoid oxidation of the UO_2 matrix during fabrication. This matrix substitution (U_3O_8 vs. UO_2) is a significant deviation with respect to the transportation rules and shipping authorization. The transportation agreement and authorization given by French Authorities only allowed Cm in a UO_2 associate matrix. So there is about a three month delay while the French Safety Authority (IRSN) conducts an investigation concerning such matrix modification. Authorization of Cm[U_3O_8] transportation should be obtained by the end of November 2007.

The first experimental results obtained in the R1-MOX configuration for oscillation of batch 1 and 2 samples are presented in Tables 15, 16, and 17 and Figures 11 and 12.

Table 15
Experimental Measurements for R1-MOX
U-235 Calibration Samples

Sample	Measurement Date	Signal (Pilot Units)	Uncertainty (Pilot Units)
H1 (0.25% U-235)	05/09/2006	1987	1210
H1 (0.25% U-235)	21/09/2006	2990	815
H1 (0.25% U-235)	25/09/2006	3399	1481
H1 (0.25% U-235)	26/09/2006	4262	2863
H1 (0.25% U-235)	28/09/2006	1935	1650
H1 (0.25% U-235)	05/10/2006	2978	1000
H1 (0.25% U-235)	25/01/2007	2199	1085
H1 (0.25% U-235)	26/01/2007	2922	889
	Average	2834	786
H2 (0.50% U-235)	05/09/2006	9703	1321
H2 (0.50% U-235)	21/09/2006	7090	1773
H2 (0.50% U-235)	25/09/2006	9021	1436

Table 15
Experimental Measurements for R1-MOX
U-235 Calibration Samples

Sample	Measurement Date	Signal (Pilot Units)	Uncertainty (Pilot Units)
H2 (0.50% U-235)	26/09/2006	9802	2404
H2 (0.50% U-235)	29/09/2006	6711	2399
H2 (0.50% U-235)	05/10/2006	9938	1172
	Average	8711	1442
H3 (0.71% U-235)	05/09/2006	20258	1920
H3 (0.71% U-235)	21/09/2006	15295	1977
H3 (0.71% U-235)	25/09/2006	15984	1710
H3 (0.71% U-235)	27/09/2006	16082	1773
H3 (0.71% U-235)	29/09/2006	13325	2072
H3 (0.71% U-235)	06/10/2006	16856	961
	Average	16300	2279
H4 (1% U-235)	05/09/2006	25639	1809
H4 (1% U-235)	22/09/2006	23545	1666
H4 (1% U-235)	25/09/2006	23537	2299
H4 (1% U-235)	27/09/2006	20872	1769
H4 (1% U-235)	29/09/2006	24314	1218
H4 (1% U-235)	06/10/2006	26100	1182
	Average		
H5 (2% U-235)	20/09/2006	56348	2172
H5 (2% U-235)	22/09/2006	53955	2483
H5 (2% U-235)	25/09/2006	52677	2210
H5 (2% U-235)	27/09/2006	55052	2521
H5 (2% U-235)	03/10/2006	52098	1711
H5 (2% U-235)	04/10/2006	52667	952
H5 (2% U-235)	06/10/2006	55184	815
	Average	53997	1590
H6 (3% U-235)	20/09/2006	82973	3024
H6 (3% U-235)	22/09/2006	79830	1998
H6 (3% U-235)	26/09/2006	83221	3251
H6 (3% U-235)	27/09/2006	78835	2167
H6 (3% U-235)	04/10/2006	80202	658
H6 (3% U-235)	06/10/2006	80690	1229
	Average	80958	1766
H7 (4% U-235)	21/09/2006	101450	2992
H7 (4% U-235)	22/09/2006	106387	2118
H7 (4% U-235)	26/09/2006	97969	2532
H7 (4% U-235)	27/09/2006	102844	2805
H7 (4% U-235)	04/10/2006	103789	1456
H7 (4% U-235)	09/10/2006	103251	778
H7 (4% U-235)	22/01/2007	104185	2253

Table 15 Experimental Measurements for R1-MOX U-235 Calibration Samples			
Sample	Measurement Date	Signal (Pilot Units)	Uncertainty (Pilot Units)
H7 (4% U-235)	24/01/2007	100885	1520
	Average	102595	2520
H8 (5% U-235)	21/09/2006	119735	2105
H8 (5% U-235)	22/09/2006	119736	2445
H8 (5% U-235)	26/09/2006	119400	3426
H8 (5% U-235)	28/09/2006	121947	2733
H8 (5% U-235)	04/10/2006	123624	964
H8 (5% U-235)	16/10/2006	121369	771
H8 (5% U-235)	31/10/2006	124826	1067
H8 (5% U-235)	12/01/2007	126783	726
H8 (5% U-235)	19/01/2007	126721	952
H8 (5% U-235)	31/01/2007	124196	2462
H8 (5% U-235)	08/02/2004	126681	993
	Average	123183	2907

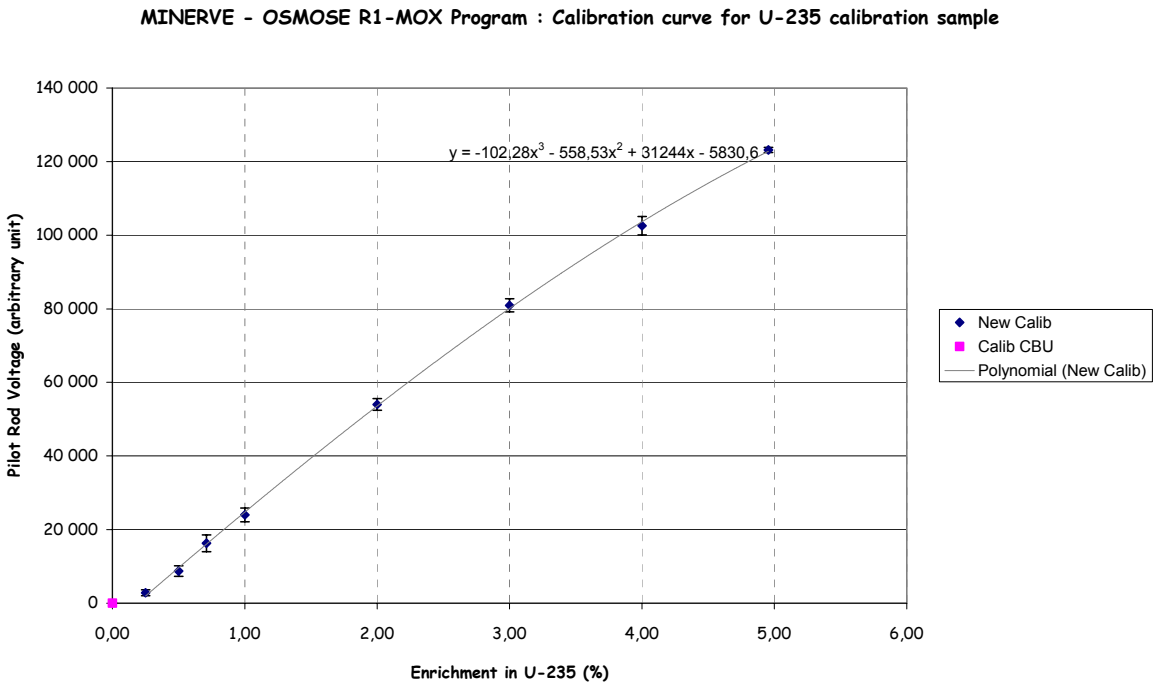

Figure 11: Calibration Curve for U-235 Samples in R1-MOX

Table 16 Experimental Measurements for R1-MOX Boron Calibration Samples			
Sample	Measurement Date	Signal (Pilot Units)	Uncertainty (Pilot Units)
10 (419 ppm)	10/10/2006	-92268	1113
10 (419 ppm)	20/11/2006	-92068	1273
10 (419 ppm)	21/11/2006	-92959	1515
10 (419 ppm)	11/01/2007	-93211	899
10 (419 ppm)	15/01/2007	-93275	1003
	Average	-92756	995
9 (150 ppm)	10/10/2006	-28659	962
9 (150 ppm)	16/11/2006	-26622	868
9 (150 ppm)	21/11/2006	-28475	1092
9 (150 ppm)	11/01/2007	-27999	1201
9 (150 ppm)	12/01/2007	-27538	547
	Average	-27858	995
7 (0 ppm)	09/10/2006	7454	788
7 (0 ppm)	16/10/2006	7877	1118
7 (0 ppm)	18/10/2006	6077	867
7 (0 ppm)	30/10/2006	8046	696
7 (0 ppm)	07/11/2006	8288	875
	Average	7548	995
34 (1062 ppm)	10/11/2006	-211698	1144
34 (1062 ppm)	21/11/2006	-207795	917
34 (1062 ppm)	11/01/2007	-213961	1012
34 (1062 ppm)	12/01/2007	-212709	938
34 (1062 ppm)	17/01/2007	-213072	975
34 (1062 ppm)	19/01/2007	-211173	1922
	Average	-211735	2170
33 (333 ppm)	10/11/2006	-68201	1009
33 (333 ppm)	20/11/2006	-70470	1435
33 (333 ppm)	11/01/2007	-68666	1226
33 (333 ppm)	12/01/2007	-68213	900
33 (333 ppm)	17/01/2007	-69652	995
	Average	-69041	995
32 (0 ppm)	09/11/2006	8539	745
32 (0 ppm)	20/11/2006	8795	1277
32 (0 ppm)	11/12/2006	7069	935
32 (0 ppm)	12/01/2007	9025	1067
32 (0 ppm)	17/01/2007	7318	644
	Average	8149	995
35 (2360 ppm)	11/10/2006	-391844	1257
35 (2360 ppm)	17/10/2006	-393596	932
35 (2360 ppm)	31/10/2006	-391725	749

Table 16 Experimental Measurements for R1-MOX Boron Calibration Samples			
Sample	Measurement Date	Signal (Pilot Units)	Uncertainty (Pilot Units)
35 (2360 ppm)	08/11/2006	-392774	953
35 (2360 ppm)	16/11/2006	-391205	1113
35 (2360 ppm)	31/01/2007	-395570	1251
35 (2360 ppm)	01/02/2007	-395738	1542
35 (2360 ppm)	12/02/2007	-395880	2135
35 (2360 ppm)	20/02/2007	-394010	848
35 (2360 ppm)	23/02/2007	-394250	1455
35 (2360 ppm)	05/03/2007	-392849	2162
	Average	-393767	1624
B500 (500 ppm)	10/10/2006	-72475	882
B500 (500 ppm)	11/10/2006	-71081	1043
B500 (500 ppm)	17/10/2006	-72657	1422
B500 (500 ppm)	31/10/2006	-71675	1165
B500 (500 ppm)	08/11/2006	-71316	1034
	Average	-71841	995
B400 (400 ppm)	11/10/2006	-57789	924
B400 (400 ppm)	17/10/2006	-57450	1159
B400 (400 ppm)	18/10/2006	-57999	1192
B400 (400 ppm)	31/10/2006	-56357	1123
B400 (400 ppm)	08/11/2006	-57958	769
	Average	-57511	995
B300 (300 ppm)	11/10/2006	-39431	971
B300 (300 ppm)	16/10/2006	-40267	1045
B300 (300 ppm)	18/10/2006	-40828	1016
B300 (300 ppm)	30/10/2006	-39807	1295
B300 (300 ppm)	08/11/2006	-40436	829
	Average	-40154	995
B200 (200 ppm)	11/10/2006	-24393	814
B200 (200 ppm)	16/10/2006	-24935	821
B200 (200 ppm)	18/10/2006	-24561	830
B200 (200 ppm)	30/10/2006	-25295	1112
B200 (200 ppm)	07/11/2006	-24322	1393
	Average	-24701	995
B100 (100 ppm)	10/10/2006	-3773	1097
B100 (100 ppm)	16/10/2006	-3344	1005
B100 (100 ppm)	18/10/2006	-3487	1100
B100 (100 ppm)	30/10/2006	-2270	902
B100 (100 ppm)	07/11/2006	-3263	1192
	Average	-3228	995

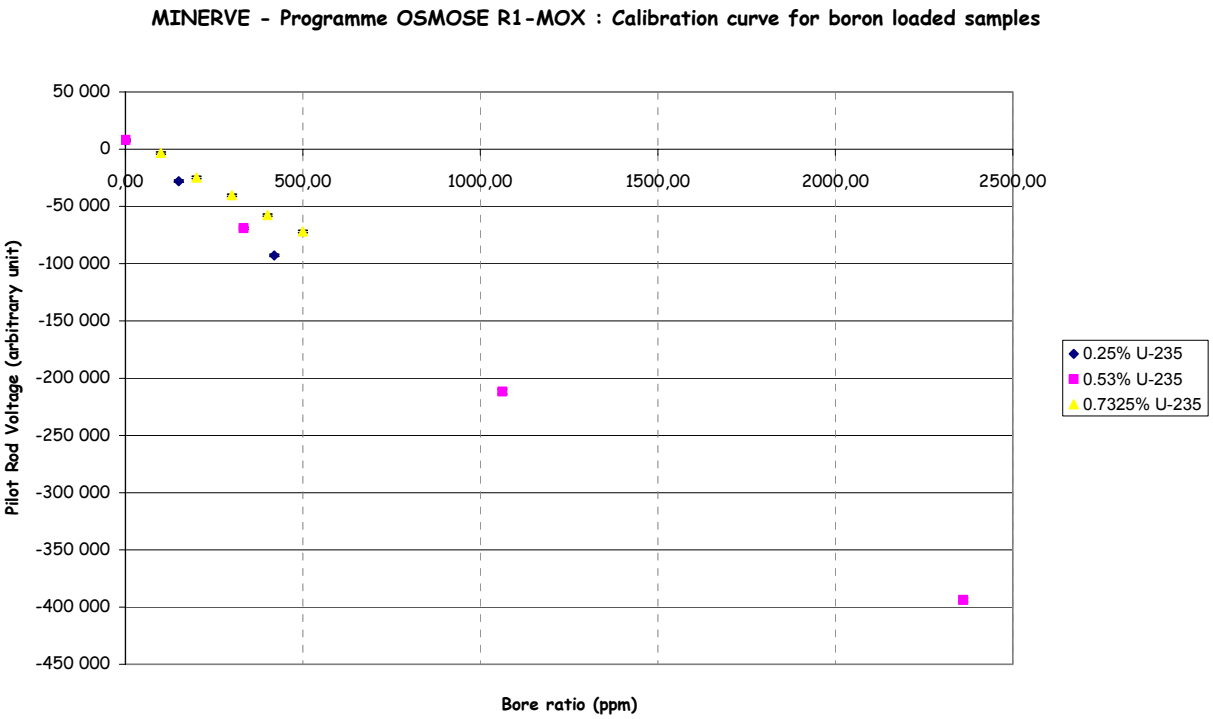

Figure 12: Calibration Curve for Boron Samples in R1-MOX

Table 17 Experimental Measurements for R1-MOX OSMOSE Samples			
Sample	Measurement Date	Signal (Pilot Units)	Uncertainty (Pilot Units)
Unat	04/10/2006	14819	1223
Unat	05/10/2006	13724	1076
Unat	09/10/2006	14055	1113
Unat	30/10/2006	15533	1262
Unat	21/11/2006	15123	1419
Unat	19/01/2007	13246	892
Unat	24/01/2007	11701	1584
Unat	29/01/2007	13310	1512
Unat	30/01/2007	14847	1102
Unat	01/02/2007	14075	1174
Unat	14/02/2007	14896	867
Unat	26/02/2007	13659	2502
	Average	14082	1055
Np237/1	24/01/2007	1007	1683
Np237/1	26/01/2007	1007	1683
Np237/1	30/01/2007	46	2231
Np237/1	01/02/2007	-108	1097

Table 17 Experimental Measurements for R1-MOX OSMOSE Samples			
Sample	Measurement Date	Signal (Pilot Units)	Uncertainty (Pilot Units)
Np237/1	07/02/2007	182	1058
	Average	427	995
Np237/2	24/01/2007	-63921	1737
Np237/2	29/01/2007	-61289	1718
Np237/2	30/01/2007	-66798	1481
Np237/2	01/02/2007	-64214	1184
Np237/2	07/02/2007	-60785	3225
Np237/2	08/02/2007	-59815	1680
	Average	-62804	2626
Th32	22/01/2007	-64441	1454
Th32	25/01/2007	-64020	1464
Th32	29/01/2007	-67888	1879
Th32	31/01/2007	-62025	1230
Th32	06/02/2007	-59118	1774
Th32	08/02/2007	-60853	2177
	Average	-63058	3086
UTh	22/01/2007	738	1991
UTh	25/01/2007	284	959
UTh	29/01/2007	-49	1741
UTh	31/01/2007	736	2164
UTh	07/02/2007	822	1452
	Average	506	995
U234	22/01/2007	-3683	1257
U234	26/01/2007	-4394	1132
U234	30/01/2007	-4704	1234
U234	31/01/2007	-4167	844
U234	07/02/2007	-2993	1482
	Average	-3988	995
URE	24/01/2007	89941	1689
URE	26/01/2007	89301	1205
URE	30/01/2007	95118	1199
URE	01/02/2007	93432	913
URE	07/02/2007	86951	2029
URE	08/02/2007	93048	1652
	Average	91298	3064
Am41/1	12/02/2007	-13331	1040
Am41/1	14/02/2007	-12625	1489
Am41/1	20/02/2007	-12573	1921
Am41/1	23/02/2007	-11353	2116
Am41/1	27/02/2007	-14301	754

Table 17 Experimental Measurements for R1-MOX OSMOSE Samples			
Sample	Measurement Date	Signal (Pilot Units)	Uncertainty (Pilot Units)
	Average	-12837	995
Am41/2	12/02/2007	-62226	1905
Am41/2	14/02/2007	-63094	1121
Am41/2	20/02/2007	-62411	2617
Am41/2	23/02/2007	-59560	1424
Am41/2	27/02/2007	-61797	1677
	Average	-61818	995
Pu238	12/02/2007	-24265	1466
Pu238	14/02/2007	-24416	1247
Pu238	20/02/2007	-22440	1365
Pu238	23/02/2007	-25028	1029
Pu238	27/02/2007	-23969	1183
	Average	-24024	995
Pu239	12/02/2007	65893	1178
Pu239	15/02/2007	64651	1563
Pu239	21/02/2007	62833	2030
Pu239	25/02/2007	66294	1368
Pu239	27/02/2007	64719	1672
	Average	64878	995

4.4. Assessment for Advanced Reactor Programs

The OSMOSE measurement campaign and program is designed as a basic study of the integral cross-sections of minor actinides. With seven different spectra available for consideration spanning from over-moderated thermal spectra to fast spectra, the entire energy range is addressed for the minor actinides. The original schedule approached the measurements in a logical progression from thermal spectra to harder spectra bootstrapping the measurement results. However, it is recognized that for high priority advanced reactor programs (such as GNEP, NGNP, and Gen-IV), the configurations need to be considered for relevance to the specific spectra and minor actinides of interest to these programs.

In the present study, calculations have been performed to investigate the similarity of the flux spectra at the sample position of different configurations with the neutron energy distributions characterizing existing thermal and fast reactors proposed under the advanced reactor programs Gen-IV, GNEP and NGNP.

4.4.1. Theoretical Approach

Besides the direct comparison of calculated values, the similarity between the investigated systems with respect to selected parameters was performed with a representativity approach as well. This methodology implies the use of sensitivity coefficients based on Generalized

Perturbation Theory (GPT) [5-7]. According to this approach, a representativity factor r_{RE} can be defined to quantify the similarity between a reactor and an experimental configuration with respect to a selected parameter [8]:

$$r_{RE} = \frac{\left(S_{I,R}^T D S_{I,E}\right)}{\left[\left(S_{I,R}^T D S_{I,R}\right)\left(S_{I,E}^T D S_{I,E}\right)\right]^{1/2}} \quad \text{Eq. 1}$$

where $S_{I,R}$ and $S_{I,E}$ are the sensitivity coefficient vectors of the parameter I under study, for the reactor and the experiment, respectively, and D is the dispersion matrix containing the nuclear data covariances. From **Eq. 1** it is observed that the parameter r_{RE} is closer to the optimum value $r_{RE} = 1$ as $S_{I,R}$ and $S_{I,E}$ become similar. The representativity factor can also be used to get an estimate of how the dispersion ΔI_1^2 in the calculation of an integral reactor parameter I is reduced, if an integral experiment E is performed:

$$\Delta I_1^2 = \Delta I_0^2\left(1 - r_{RE}^2\right), \quad \text{Eq. 2}$$

where ΔI_0^2 is the original dispersion:

$$\Delta I_0^2 = S_{I,R}^T D S_{I,R}\,. \quad \text{Eq. 3}$$

In addition to k_{eff}, in the present study a representativity analysis is performed with respect to the parameter $\eta=\nu\Sigma_f\Phi/\Sigma_a\Phi$ calculated at the sample location of the experimental configurations and in relevant core positions of actual thermal and fast reactors. In addition to the study of flux spectrum similarities, the parameter η has been also selected for another purpose: if $\nu\Sigma_f$ and Σ_a are the sample cross-sections, it would be perhaps possible to get information on the performed measurements of the reactivity changes subsequent to the sample substitution in the OSMOSE configurations.

The formulas for the k_{eff} and η sensitivity coefficients are presented in the following:

$$S_k = \frac{\partial k}{\partial \sigma}\cdot\frac{\sigma}{k} = -\frac{k}{I_f}\left\{\left\langle \Phi^*, \left(\frac{\partial A}{\partial \sigma} - \frac{1}{k}\frac{\partial F}{\partial \sigma}\right)\Phi\right\rangle\right\} \quad \text{Eq. 4}$$

$$S_\eta = \frac{\sigma}{\eta}\frac{d\eta}{d\sigma} = \frac{\sigma}{\eta}\left\{\frac{\partial \eta}{\partial \sigma} - \left\langle \Psi^*, \left(\frac{\partial A}{\partial \sigma} - \frac{1}{k}\frac{\partial F}{\partial \sigma}\right)\Phi\right\rangle\right\} = \left\{S_{\eta,D} - S_{\eta,I}\right\} \quad \text{Eq. 5}$$

where ψ^* is the importance function solution of the equation:

$$\left(A^* - \frac{1}{k}F^*\right)\tilde{\Psi}^* = \frac{1}{\eta}\frac{\partial \eta}{\partial \Phi} = \frac{\nu\Sigma_f(\vec{r},E)}{\langle \nu\Sigma_f\Phi\rangle} - \frac{\Sigma_a(\vec{r},E)}{\langle \Sigma_a\Phi\rangle} \quad \text{Eq. 6}$$

with $\tilde{\Psi}^* = \frac{\Psi^*}{\eta}$. Additionally, in **Eq. 5**:

$$S_{\eta,D} = \frac{\sigma}{\eta}\cdot\frac{\partial \eta}{\partial \sigma} = \left(S_{\eta,D}\right)_{i,g,d} = \frac{\sigma}{\eta}\left(\frac{\left(\langle \nu\Sigma_f\Phi\rangle\right)_{i,g}}{\langle \nu\Sigma_f\Phi\rangle} - \frac{\left(\langle \Sigma_a\Phi\rangle\right)_{i,g,d}}{\langle \Sigma_a\Phi\rangle}\right)_{\substack{i=\text{isotope}\\ g=\text{energy group}\\ d=\text{reactor domain}}} \quad \text{Eq. 7}$$

is the direct term of the sensitivity coefficients accounting of the variations on η directly due to the variations of detector cross-sections $\nu\Sigma_f$ and Σ_a. In the present study, the direct term $S_{\eta,D}$ has been neglected assuming that no variation is associated with the detector cross-sections. $S_{\eta,I}$ is the indirect term of the sensitivity coefficients, accounting for the variations on η due to the change in the flux spectrum determined by the cross-section variations.

4.4.2. Systems under Study

The OSMOSE configurations considered in the present analysis are characterized by four different lattices aiming at reproducing a typical PWR (R1-UO_2 configuration), an over-moderated UO_2 (R2-UO_2), a PWR MOX (R1-MOX), and an epithermal (MORGANE-R, MR) spectrum at the center of the MINERVE cores.

The representativity study has been performed with respect to the same reactors recently investigated within the OECD Subgroup 26 for an extensive uncertainty/target accuracy assessment in order to define priority needs in nuclear data improvements [9]: an Advanced Burner Test Reactor (ABTR), a Sodium-cooled Fast Reactor (SFR), a large sodium-cooled fast reactor, referred as EFR, a Gas-cooled Fast Reactor (GFR), a Lead-cooled Fast Reactor (LFR), an Accelerator-Driven System (ADS), and an extended burnup (100 GWd/t) Pressurized Water Reactor (PWR). The main features of each reactor are recalled as follows:

1. ABTR: 250 MW_{th} – Na cooled; U-TRU-10Zr fuel; HT9(75%)-Na(15%) reflector; enrichment: 17%, MA: <1%; irradiation cycle: 109.8 days (4 months at 90% capacity);
2. SFR: (Burner: CR=0.25) 840 MW_{th} – Na cooled; U-TRU-Zr metallic alloy fuel; SS reflector; enrichment: 56%, MA: 10%; irradiation cycle: 155 days;
3. EFR: 3600 MW_{th} – Na cooled; U-TRU oxide fuel; U blanket; enrichment: 22%, MA: 1%; irradiation cycle: 1700 days;
4. GFR: 2400 MW_e – He cooled; SiC - (U-TRU)C fuel; Zr_3Si_2 reflector; enrichment: 17%, MA: 5%; irradiation cycle: 415 days;
5. LFR: 900 MW_{th} – Pb cooled; U-TRU-Zr metallic alloy fuel; Pb reflector; enrichment: 21%, MA: 2%; irradiation cycle: 310 days;
6. ADS: 377 MW_{th} – Pb-Bi cooled; TRU fuel; HT9(70%) Pb-Bi(30%) reflector; enrichment: 32%, MA: 67%; irradiation cycle: 366 days;
7. Extended BU PWR: enrichment: 8.5%; burnup: 100 GW d/Kg.

4.4.3. Computational Tools and Strategies

All the sensitivity calculations were performed with the ERANOS code system [10], which allows one to calculate homogeneous and inhomogeneous solutions of the Boltzmann equations, generalized importance functions, and to perform perturbation and uncertainty analysis. The discrete ordinate module BISTRO [11] has been used to perform flux and generalized importance function calculations.

Flux spectra, η values and k_{eff} sensitivity coefficients have been calculated in S_4P_1 transport approximation, except for the LFR where the complete study has been performed in diffusion theory, due to convergence problems encountered in transport theory approximations. For all systems, the sensitivity coefficients related to η have been calculated using diffusion approximations which have been proved accurate enough for this type of analysis.

Cross-section data have been processed with the ECCO code [12] using the JEF3.1 library [13]. For most of the investigated reactors (except the ABTR and the PWR), homogenized cross-sections have been calculated, since heterogeneity effects on the cross-sections are rather small for the kind of study intended to be performed. For an accurate description of the neutron

slowing down in thermal systems, the cross-sections have been produced over a 172 energy group structure.

4.4.4. Flux Spectra and η Calculated Values

Due to the features of the OSMOSE configurations, the study is performed only for the central region surrounding the sample location, in XY geometry, with reflection boundary conditions and an opportune buckling in order to characterize the leakage. The reactor zones outside the selected region do not have a significant impact on the neutron energy distribution at the core center, where the samples are located. On the other hand, the calculation models used for the study of the selected reactors are consistent with those adopted in the previous studies [9]. Table 18 summarizes the calculated k_{eff} of each investigated system.

Table 18: Calculated k_{eff} (Reactivity) of the OSMOSE Configurations and Reactors	
OSMOSE Configurations	
R1-UO2	0.999976 (-2.4 pcm)
R2-UO2	0.999982 (-1.8 pcm)
R1-MOX	0.999958 (-4.2 pcm)
MORGANE-R	1.000021 (2.1 pcm)
Advanced Reactor Configurations	
ABTR	1.04295 (4118.1 pcm)
SFR	1.065548 (6151.6 pcm)
EFR	1.115667 (10367.5 pcm)
GFR	1.015783 (1553.8 pcm)
LFR	1.025412 (2478.2 pcm)
ADS	0.978075 (-2241.6 pcm)
PWR	1.52869 (34584.5 pcm)

The initial analysis has been devoted to the energy distribution of the direct and adjoint fluxes. The flux spectra have been calculated at the core center, except for the few reactors (like the ABTR) where at that position a control rod is in place. In this case, an opportune point of the inner core, far from spectral perturbations induced by the central assembly, was selected for the calculation. For the OSMOSE configurations, the fluxes have been calculated without a sample in place (at the sample position there is only water). For further details on the models and results see the report on OSMOSE Representativity Studies [14].

The flux spectra are presented in Figures 13 to 34 for each system under study. It can be observed that for all fast reactors, the fraction of neutrons below 1 keV is practically negligible and the peak of the distribution is at ~100 – 200 keV. In the case of the OSMOSE configurations, the flux spectra below 1 keV is still relevant. As expected, the R1-UO_2 and R2-UO_2 configurations show a peak in the thermal energy range. Additionally, for the four OSMOSE configurations the peak of the distributions is at ~1 MeV and it becomes more pronounced in the case of R1-MOX and MR configurations. Finally, the OSMOSE flux spectra look much more

similar to PWR spectra (especially in the case of the R1-UO_2 and R2-UO_2 configurations) than to the neutron energy distributions typical of fast systems.

In addition to the neutron flux spectra, calculations have been also performed for the parameter η. The parameter $\eta=\nu\Sigma_f\Phi/\Sigma_a\Phi$ is calculated with the macroscopic cross-sections $\nu\Sigma_f$ and Σ_a of the sample pin in a heterogeneous cell calculation, while the fluxes are obtained from the reactor and experimental configuration models without a sample in place and calculated at the same locations of the neutron spectrum distributions previously discussed. Table 19 shows the results for the parameter η.

Table 19
Calculated η

Sample	R1-UO_2	R2-UO_2	R1-MOX	MR			
Th232	0.0430	0.0394	0.0670	0.0926			
UTh	0.7559	0.7770	0.5751	0.4653			
U234	0.7547	0.7733	0.5843	0.4825			
URE	1.5135	1.5441	1.2291	0.9168			
UO_2	0.8216	0.8401	0.6329	0.5140			
Np237_1	0.7801	0.7993	0.6038	0.4969			
Np237_2	0.6269	0.6473	0.4960	0.4308			
Pu238	0.8126	0.8163	0.6815	0.5737			
Pu239	1.4412	1.4600	1.1950	0.8852			
Pu240	0.5471	0.5782	0.4846	0.4331			
Pu241	1.1015	1.1227	0.8418	0.6349			
Pu242	0.6997	0.7269	0.5310	0.4351			
Am241_1	0.7373	0.7561	0.5869	0.4916			
Am241_2	0.5973	0.6154	0.5041	0.4485			
Sample	ABTR	SFR	EFR	GFR	LFR	ADS	PWR
Th232	0.1210	0.0865	0.0764	0.0757	0.0831	0.0923	0.0624
UTh	0.6334	0.4960	0.4656	0.4761	0.4891	0.5128	0.6885
U234	0.6755	0.5327	0.5005	0.5126	0.5273	0.5503	0.6928
URE	0.9424	0.8165	0.7870	0.7940	0.8312	0.8250	1.3795
UO_2	0.6605	0.5215	0.4915	0.5054	0.5105	0.5362	0.7585
Np237_1	0.6631	0.5227	0.4918	0.5047	0.5142	0.5389	0.7175
Np237_2	0.6750	0.5284	0.4930	0.5017	0.5315	0.5516	0.5703
Pu238	0.7720	0.6228	0.5861	0.5936	0.6320	0.6412	0.7904
Pu239	0.8428	0.6918	0.6521	0.6547	0.7127	0.7073	1.3547
Pu240	0.6726	0.5309	0.4995	0.5125	0.5231	0.5473	0.4699
Pu241	0.7034	0.5652	0.5353	0.5483	0.5582	0.5786	1.0084
Pu242	0.6878	0.5418	0.5079	0.5200	0.5387	0.5616	0.6183
Am241_1	0.6611	0.5216	0.4913	0.5049	0.5115	0.5372	0.6815
Am241_2	0.6626	0.5222	0.4908	0.5040	0.5139	0.5396	0.5537

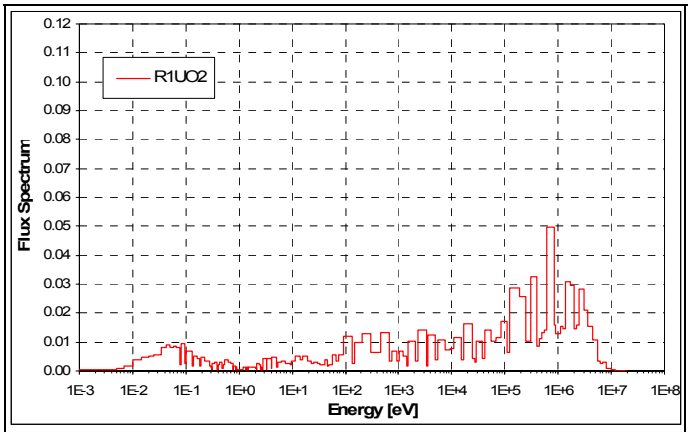

Figure 13: OSMOSE R1-UO2 Direct Flux Spectrum

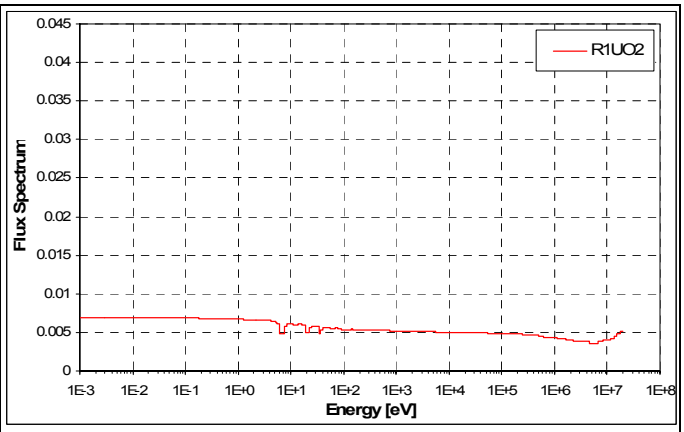

Figure 14: OSMOSE R1-UO2 Adjoint Flux Spectrum

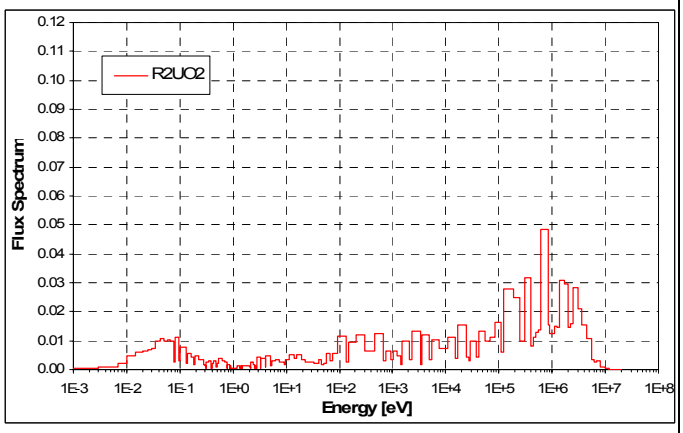

Figure 15: OSMOSE R2-UO2 Direct Flux Spectrum

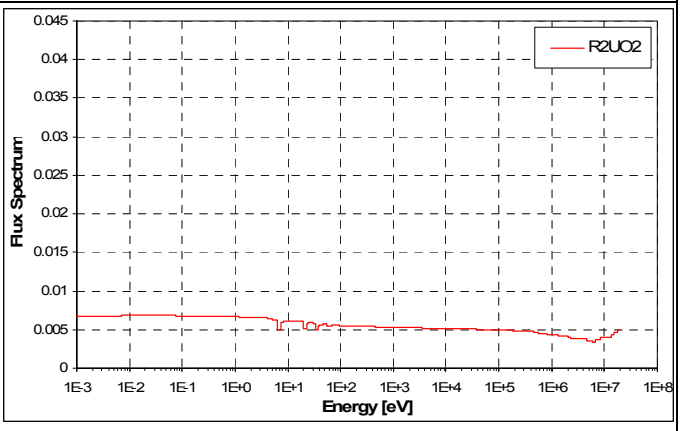

Figure 16: OSMOSE R2-UO2 Adjoint Flux Spectrum

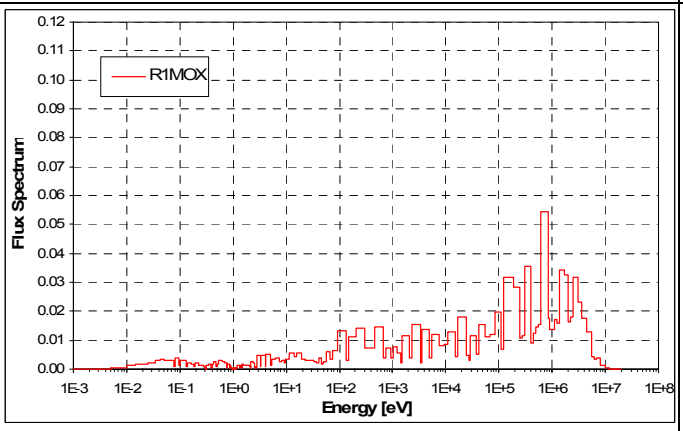

Figure 17: OSMOSE R1-MOX Direct Flux Spectrum

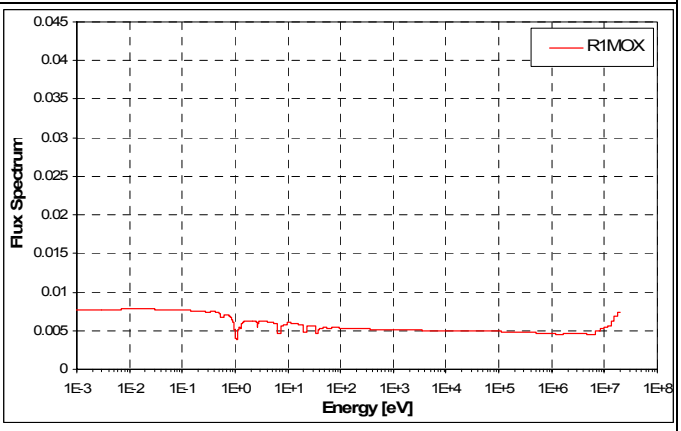

Figure 18: OSMOSE R1-MOX Adjoint Flux Spectrum

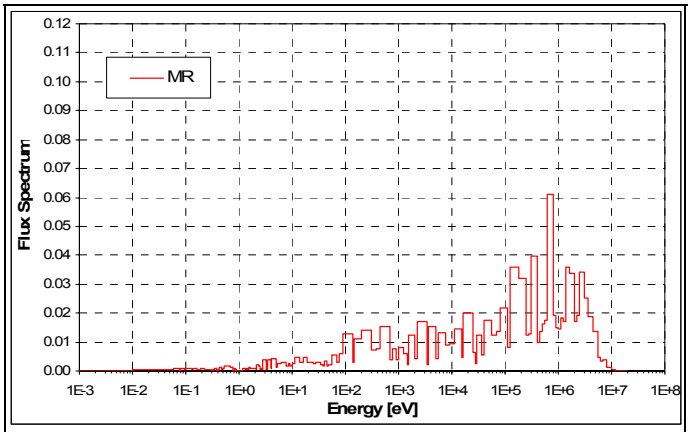

Figure 19: OSMOSE MORGANE/R Direct Flux Spectrum

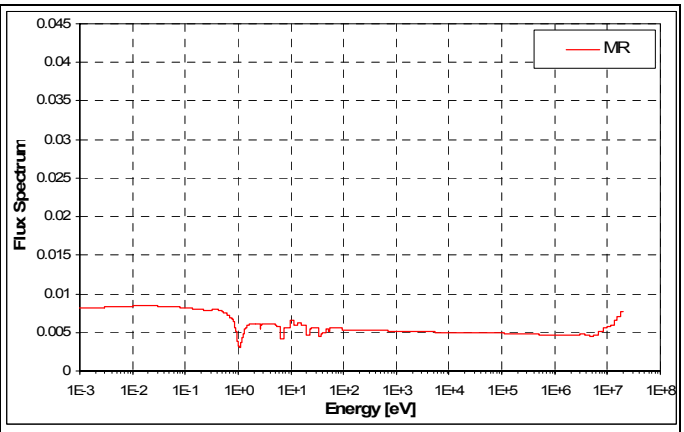

Figure 20: OSMOSE MORGANE/R Adjoint Flux Spectrum

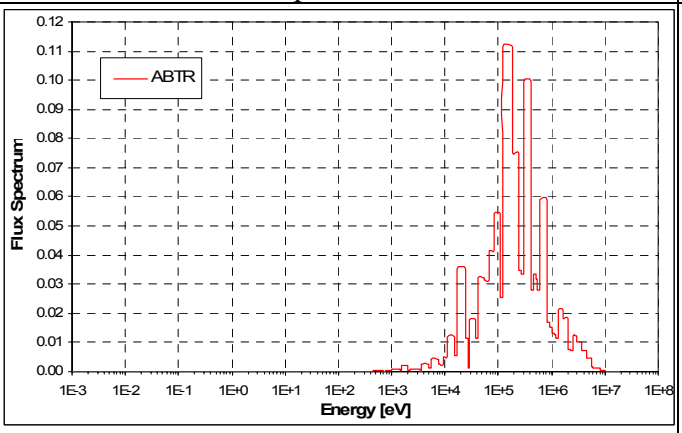

Figure 21: ABTR Direct Flux Spectrum

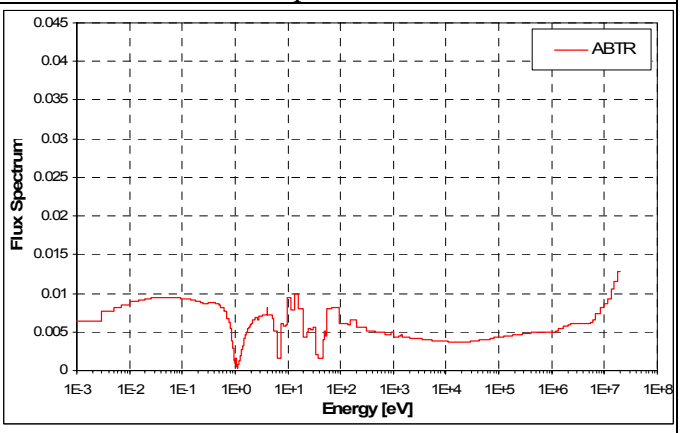

Figure 22: ABTR Adjoint Flux Spectrum

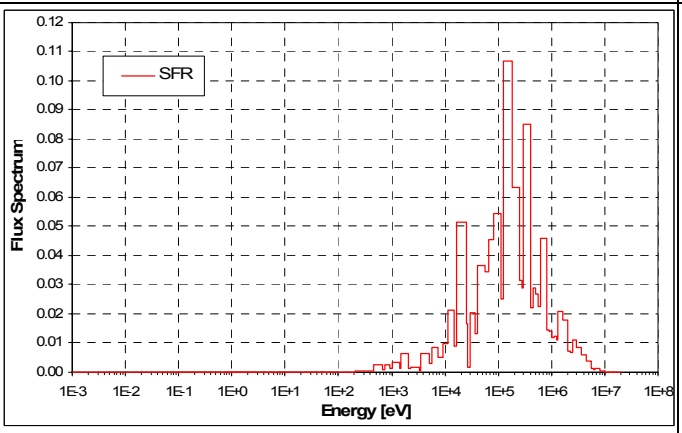

Figure 23: SFR Direct Flux Spectrum

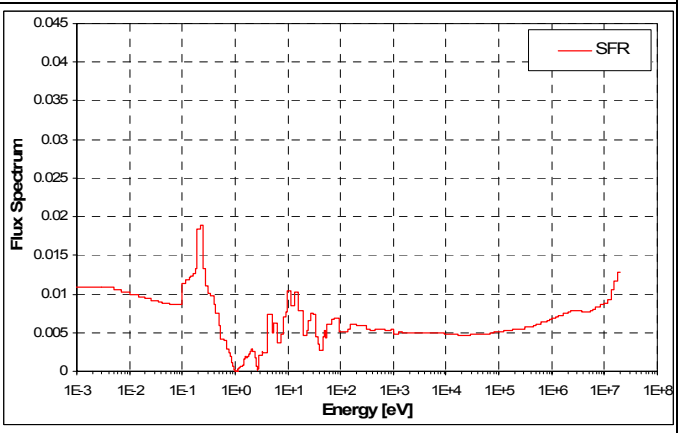

Figure 24: SFR Adjoint Flux Spectrum

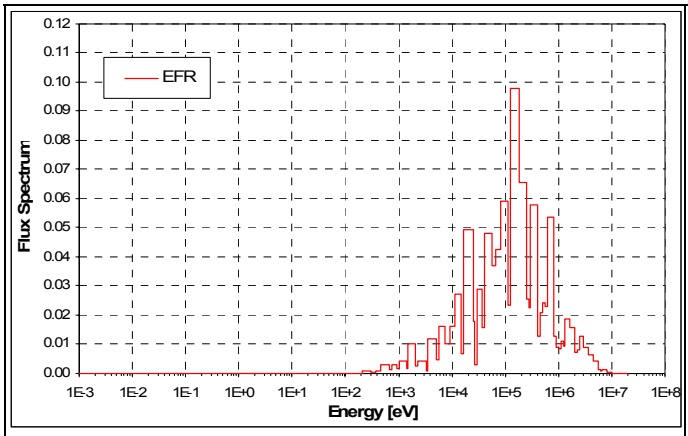

Figure 25: EFR Direct Flux Spectrum

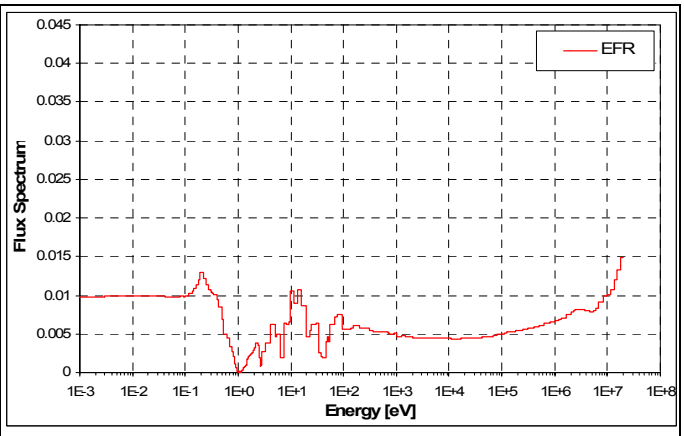

Figure 26: EFR Adjoint Flux Spectrum

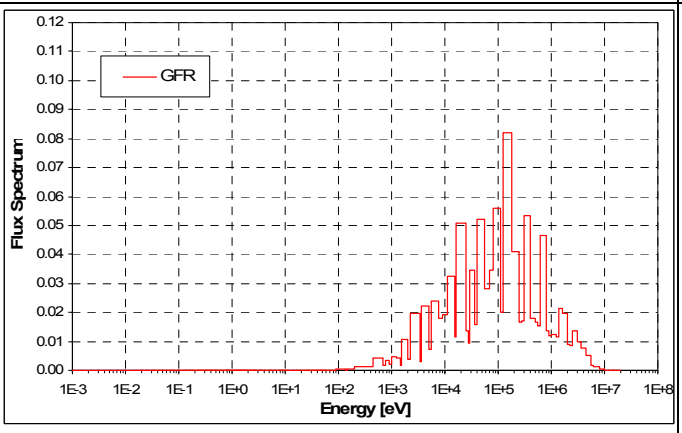

Figure 27: GFR Direct Flux Spectrum

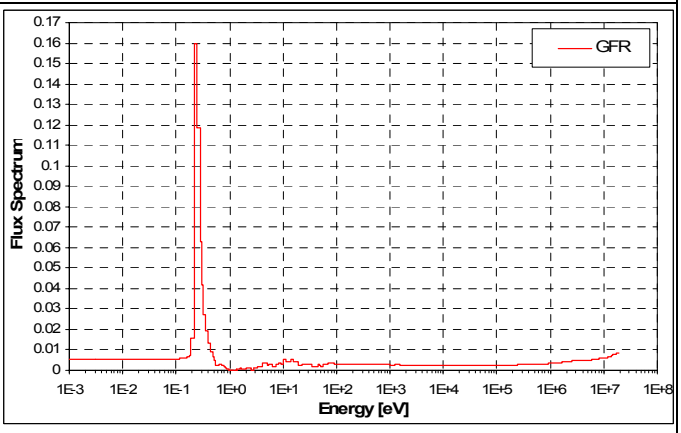

Figure 28: GFR Adjoint Flux Spectrum

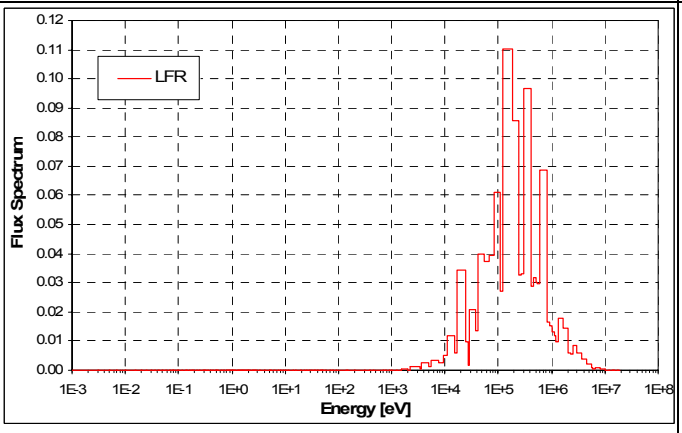

Figure 29: LFR Direct Flux Spectrum

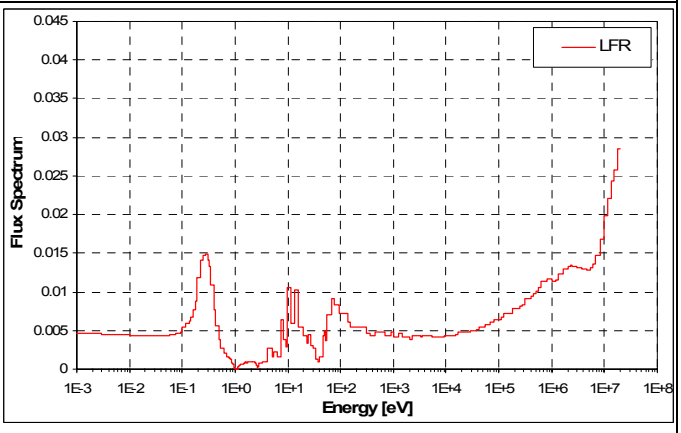

Figure 30: LFR Adjoint Flux Spectrum

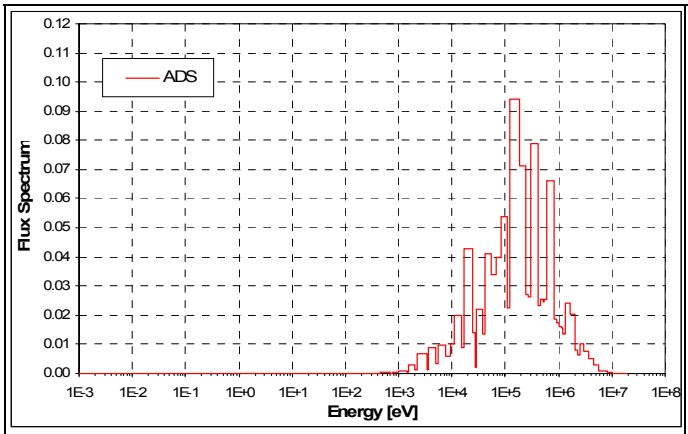

Figure 31: ADS Direct Flux Spectrum

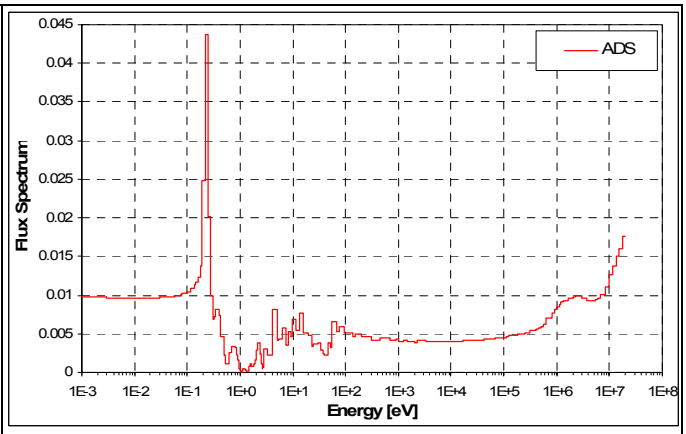

Figure 32: ADS Adjoint Flux Spectrum

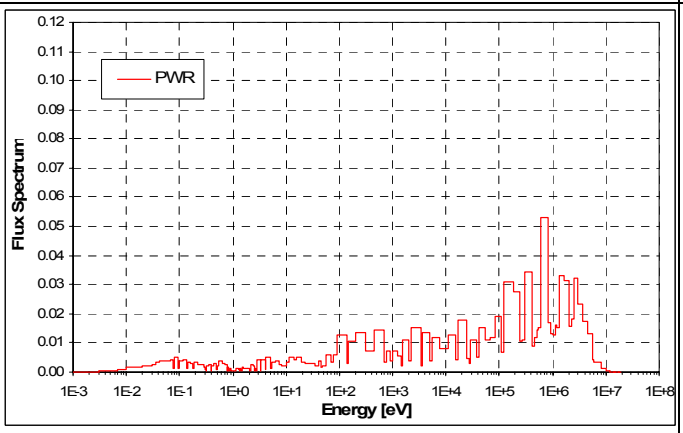

Figure 33: PWR Direct Flux Spectrum

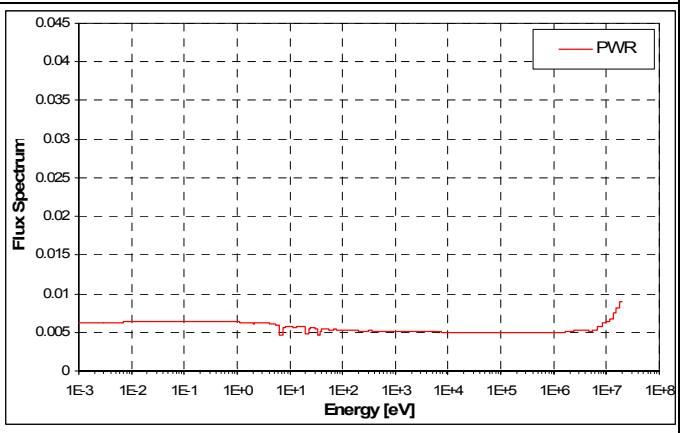

Figure 34: PWR Adjoint Flux Spectrum

4.4.5. Representativity Analysis

A representativity study has been performed between the OSMOSE configurations and the selected reactors with respect to the multiplication factors and the parameters η previously calculated.

Due to the unavailability of nuclear data covariance over the adopted 172 energy group structure, the representativity study has been performed without the use of a dispersion matrix: this is obtained by setting D equal the unity matrix in **Eq. 1**. As a consequence, the present representativity analysis is based on the direct comparison of sensitivity profiles, without any filter due to specific nuclear data uncertainties: this is a good approach for deriving general conclusions that are not related to a specific data library.

Table 20 shows the representativity factors for k_{eff}, while in [14] the sensitivity coefficients are presented by isotope, energy group and cross-section type for each system under study. It can be observed that low representativity factors are obtained in general with respect to k_{eff} between the OSMOSE configurations and all fast reactors, while a good representativity is shown as expected between the R1-UO_2 or R2-UO_2 configuration and the PWR. Looking at the sensitivity coefficients, it is observed for the OSMOSE configurations, besides the U-235 (case of R1-UO2

Table 20:
Representativity Factors Between
OSMOSE and Reactors for k_{eff}

	R1-UO_2	**R2-UO_2**	**R1-MOX**	**MR**
R1-UO_2	-	0.9981	0.2476	0.1586
R2-UO_2	0.9981	-	0.2318	0.1421
R1-MOX	0.2476	0.2318	-	0.8710
MR	0.1586	0.1421	0.8710	-
ABTR	0.0293	0.0261	0.0712	0.1826
SFR	0.0131	0.0116	0.0493	0.1549
EFR	0.0355	0.0313	0.0843	0.2101
GFR	0.0547	0.0481	0.1125	0.2434
LFR	0.0251	0.0223	0.0632	0.1655
ADS	-0.0001	-0.0001	0.0254	0.1072
PWR	0.9479	0.9337	0.2390	0.1522

and R2-UO_2) or Pu-239 (case of R1-MOX and MR), an important role is also played by the hydrogen. For the fast reactors, the sensitivity profiles are practically always dominated by the Pu-239 components (in the case of the SFR the Minor Actinides (MA) contributions are also significant). The PWR shows sensitivity profiles very similar to those calculated for OSMOSE R1-UO_2 and R2-UO_2.

Tables 21-24 show the representativity factors for the parameter η. As in the case of the multiplication factor, low representativity factors are obtained in general with respect to the parameter η between the OSMOSE configurations and all fast reactors, while a good representativity is shown as expected between the R1-UO_2 or R2-UO_2 configuration and the PWR. Looking at the sensitivity coefficients, it is observed that besides the fissile isotopes U-235 (case of R1-UO_2, R2-UO_2 and PWR), Pu-239 (case of R1-MOX, MR and all fast reactors) and minor actinides (case of SFR and ADS), a significant role (dominant in most of the cases) is played by the structural isotopes, as H (case of R1-UO_2, R2-UO_2 and PWR), Fe-56 (case of ABTR, SFR, EFR, ADS), Na-23 (case of ABTR, SFR, EFR), O-16 (case of EFR), C and Si-28 (case of GFR), Pb isotopes and B-10 (case of LFR). In fact, the fissile isotope sensitivity coefficients related to the fission reaction contribute to the numerator (for the production, with ν) and to the denominator (for the absorption, with $\Sigma_a = \Sigma_c + \Sigma_f$) of the parameter η with opposite sign, weakening as consequence the total effect.

Table 21:
Representativity Factors Between OSMOSE R1-UO_2 and Reactors for η

Sample	ABTR	SFR	EFR	GFR	LFR	ADS	PWR
Th232	0.1952	0.0704	0.2474	0.2099	0.1630	0.0130	0.9448
UTh	0.0549	0.0197	0.0688	0.0581	0.0453	0.0035	0.9659
U234	0.0582	0.0210	0.0734	0.0619	0.0479	0.0037	0.9600
URE	0.0137	0.0048	0.0174	0.0147	0.0109	0.0009	0.9836
UO_2	0.0539	0.0193	0.0676	0.0567	0.0444	0.0035	0.9666
Np237_1	0.0574	0.0206	0.0721	0.0607	0.0472	0.0037	0.9634
Np237_2	0.0704	0.0257	0.0895	0.0762	0.0580	0.0045	0.9523
Pu238	0.0570	0.0206	0.0728	0.0618	0.0464	0.0036	0.9699
Pu239	0.0169	0.0060	0.0214	0.0184	0.0135	0.0011	0.9800
Pu240	0.0524	0.0188	0.0659	0.0555	0.0432	0.0033	0.9649
Pu241	0.0328	0.0117	0.0412	0.0346	0.0268	0.0021	0.9779
Pu242	0.0489	0.0177	0.0617	0.0523	0.0402	0.0031	0.9645
Am241_1	0.0619	0.0222	0.0777	0.0653	0.0510	0.0040	0.9598
Am241_2	0.0749	0.0270	0.0942	0.0795	0.0619	0.0048	0.9493

Table 22:
Representativity Factors Between OSMOSE R2-UO_2 and Reactors for η

Sample	ABTR	SFR	EFR	GFR	LFR	ADS	PWR
Th232	0.1772	0.0639	0.2266	0.1902	0.1480	0.0118	0.9297
UTh	0.0428	0.0154	0.0542	0.0453	0.0353	0.0028	0.9530
U234	0.0456	0.0165	0.0581	0.0485	0.0375	0.0029	0.9431
URE	0.0107	0.0038	0.0137	0.0115	0.0085	0.0007	0.9754
UO_2	0.0418	0.0150	0.0530	0.0440	0.0345	0.0027	0.9543
Np237_1	0.0446	0.0160	0.0565	0.0471	0.0367	0.0029	0.9499
Np237_2	0.0554	0.0202	0.0711	0.0599	0.0456	0.0035	0.9329
Pu238	0.0456	0.0164	0.0588	0.0494	0.0371	0.0029	0.9575
Pu239	0.0133	0.0047	0.0171	0.0145	0.0107	0.0009	0.9689
Pu240	0.0424	0.0153	0.0538	0.0449	0.0350	0.0027	0.9449
Pu241	0.0255	0.0091	0.0324	0.0268	0.0209	0.0017	0.9692
Pu242	0.0396	0.0143	0.0504	0.0423	0.0326	0.0025	0.9417
Am241_1	0.0481	0.0173	0.0609	0.0507	0.0396	0.0031	0.9449
Am241_2	0.0591	0.0213	0.0749	0.0626	0.0487	0.0038	0.9286

Table 23:
Representativity Factors Between OSMOSE R1-MOX and Reactors for η

Sample	ABTR	SFR	EFR	GFR	LFR	ADS	PWR
Th232	0.1976	0.0748	0.2421	0.2104	0.1659	0.0290	0.9302
Uth	0.0950	0.0357	0.1154	0.0993	0.0791	0.0132	0.9117
U234	0.0974	0.0368	0.1188	0.1022	0.0809	0.0135	0.9131
URE	0.0281	0.0103	0.0342	0.0290	0.0226	0.0039	0.7990
UO_2	0.0925	0.0347	0.1123	0.0960	0.0769	0.0129	0.9158
Np237_1	0.0972	0.0366	0.1183	0.1015	0.0808	0.0135	0.9103
Np237_2	0.1152	0.0440	0.1415	0.1231	0.0957	0.0159	0.8918
Pu238	0.0859	0.0324	0.1058	0.0918	0.0705	0.0119	0.9218
Pu239	0.0315	0.0117	0.0384	0.0330	0.0255	0.0044	0.8302
Pu240	0.1134	0.0427	0.1380	0.1185	0.0943	0.0157	0.6938
Pu241	0.0625	0.0234	0.0759	0.0645	0.0517	0.0087	0.8783
Pu242	0.0921	0.0349	0.1125	0.0972	0.0765	0.0127	0.8929
Am241_1	0.1013	0.0381	0.1231	0.1054	0.0842	0.0141	0.9092
Am241_2	0.1183	0.0447	0.1440	0.1240	0.0985	0.0163	0.8866

Table 24:
Representativity Factors Between OSMOSE MR and Reactors for η

Sample	ABTR	SFR	EFR	GFR	LFR	ADS	PWR
Th232	0.2622	0.1405	0.3216	0.2658	0.2106	0.0466	0.9190
UTh	0.2040	0.1066	0.2485	0.2052	0.1637	0.0344	0.8856
U234	0.2032	0.1063	0.2482	0.2051	0.1625	0.0340	0.8884
URE	0.0921	0.0466	0.1119	0.0924	0.0718	0.0151	0.7697
UO_2	0.1993	0.1040	0.2426	0.1988	0.1597	0.0336	0.8916
Np237_1	0.2047	0.1070	0.2496	0.2054	0.1640	0.0344	0.8873
Np237_2	0.2236	0.1176	0.2748	0.2302	0.1788	0.0370	0.8606
Pu238	0.1790	0.0931	0.2203	0.1843	0.1417	0.0295	0.9025
Pu239	0.0942	0.0482	0.1148	0.0960	0.0738	0.0155	0.8079
Pu240	0.2232	0.1166	0.2724	0.2244	0.1788	0.0374	0.6106
Pu241	0.1622	0.0843	0.1974	0.1616	0.1295	0.0273	0.8518
Pu242	0.1939	0.1016	0.2373	0.1971	0.1552	0.0321	0.8590
Am241_1	0.2078	0.1086	0.2531	0.2079	0.1666	0.0349	0.8881
Am241_2	0.2239	0.1172	0.2732	0.2255	0.1796	0.0375	0.8556

5. Summary

The OSMOSE experimental program, carried out at the MINERVE facility of CEA-Cadarache, aims at producing very accurate reactivity-sample worth measurements for a series of actinides in various spectra, from very thermalized to very fast. The activities are divided into five high-level tasks: reactor modeling and pre-experiment analysis, sample fabrication and analysis, reactor experiments, data treatment and analysis, and assessment for relevance to high priority advanced reactor programs (such as GNEP and Gen-IV).

Progress in 2007 on each task was described in detail in the previous sections and is summarized here.

Reactor modeling and analysis for pre-experiment planning was performed for two reactor configurations – the R2-UO2 configuration (representative of an overmoderated thermal spectrum) and the MORGANE-R configuration (representative of a thermal spectrum with a large epithermal component). These are the next two configurations that are scheduled for experimental measurements in the MINERVE facility in 2008.

OSMOSE sample pellet fabrication and analysis (isotopic composition vs mass ratio) was completed for the first two sample batches (except for ThO2) in the first quarter of 2006 and the second quarter of 2007 respectively.

The last set of pellets is composed of five samples: UO_2 + $^{233}UO_2$; UO_2 + $^{243}AmO_2$; U_3O_8 + $^{244}CmO_2$; U_3O_8 + $^{244+245}CmO_2$ and finally the U_3O_8 reference. The OSMOSE furnace and the uniaxial three-part die were used during the fabrication of the third set of samples. For the samples containing Cm, it was decided not to sinter the pellets with curium isotopes because of the lack of radioprotection of the OSMOSE furnace. As a consequence, a new press was installed in a hot cell of the ATALANTE C10 line which is suitable for the fabrication and the study of high neutron activity compounds. The green pellets for two samples (^{244}Cm and $^{244+245}$Cm doped compound) and a set of uranium sesquioxide for calibration were fabricated.

To help reduce uncertainties associated with the experimental results, ANL is providing post-fabrication destructive analysis of selected OSMOSE sample pellets for isotopic composition and impurities. The ANL sample-analysis activity involves providing corroborative compositional data for one pellet composed of isotopically natural UO_2, and eight pellets composed of the natural uranium matrix doped with specific minor-actinide isotopes [U-234, Th-232, Pu-240, Pu-242, Np-237 (2 levels) and Am-241 (2 levels)]. For the natural uranium pellet, ANL is determining the uranium assay, the uranium isotopic composition, and the concentrations of "absorber" and "banal" impurities.

After a shipping delay while authorizations were pending from Safety Authorities in France, the OSMOSE sample pellets were delivered to ANL in December 2006 and the shipping container was returned to CEA.

The analysis of the natural uranium pellet to determine the uranium mass fraction, uranium isotopic composition, and select impurity elements has been completed. Measurements with the

Th-232 and U-234 doped pellets have also been completed. The Pu-240 and Pu-242 doped pellets have been processed and prepared samples are in hand for mass spectrometric analysis to determine (1) the plutonium isotopic composition and mass fraction (by isotope dilution), and (2) the uranium mass fraction, in each pellet.

The schedule for conduct of OSMOSE measurements in the MINERVE facility is dictated by commitments for facility operations for several programs at CEA-Cadarache. The R1-MOX configuration was previously loaded in MINERVE in July 2006. Calibration samples were oscillated from September 2006 to January 2007. The first and second batches of OSMOSE samples were then oscillated in the R1-MOX configuration from January 2007 to March 2007. The third batch of OSMOSE samples will be oscillated in MINERVE by December 2007.

In order to qualify the relevant experimental configurations for the achievement of the proposed goals, calculations were performed to investigate the similarity of the flux spectra of the OSMOSE configurations with the neutron energy distributions characterizing existing thermal and fast reactors proposed under the advanced reactor programs Gen-IV, GNEP and NGNP. From the direct comparison of the flux spectra calculated at the core center, it was observed that for the fast reactors, the fraction of neutrons below 1 keV is practically negligible and the peak of the distribution is at ~100–200 keV. In the case of the OSMOSE configurations, the flux spectra below 1 keV is still relevant and the peak of the distributions is at ~1 MeV (becoming more pronounced in the case of R1-MOX and MORGANE/R configurations). It was concluded that the OSMOSE flux spectra look much more similar to PWR spectra than to the spectra typical of fast systems.

The direct comparison of the flux spectra is not completely appropriate to quantify the relevance of the proposed experimental configurations for their similarity with actual reactors. For this purpose, a representativity study was carried out based on the comparison of sensitivity profiles associated with the integral parameters of interest. In addition to k_{eff}, a representativity analysis was performed with respect to the parameter $\eta=\nu\Sigma_f\Phi/\Sigma_a\Phi$ calculated at the sample location of the experimental configurations and in relevant core positions of the actual thermal and fast reactors. The parameter η is calculated with the sample cross-sections $\nu\Sigma_f$ and Σ_a.

Low representativity factors (<0.2 on a scale from 0 to 1) were obtained in general with respect to k_{eff} and the parameter η between the OSMOSE configurations and all fast reactors, while a high representativity is shown as expected between the R1-UO_2 or R2-UO_2 configuration and the PWR. The obtained results lead to the conclusion that the reactivity worth measurements obtained from the R1-MOX and MORGANE/R configurations are not to be intended as measured in flux spectra characterizing actual fast reactors. It is expected that the additional configurations possible in MINERVE would be much more representative of fast reactors as they were designed to address harder neutron spectra. However, representativity calculations for these configurations were not performed as these configurations are not part of the OSMOSE program.

6. References

1. Z. Zhong and R.Klann, Reactivity-Worth Estimates of the OSMOSE Samples in the MINERVE Reaction R1-MOX, R2-UO2, and MORGANE/R Configurations, Argonne National Laboratory Technical Report, ANL-AFCI-196, July 23, 2007.

2. G. Marleau, A. Hebert, and R. Roy, A User Guide for the DRAGON 3.05B, IGE-174, Rev. 6B, June 2006.

3. Z. Zhong, R. Klann, and G. Stoven, Results of Calculations for the OSMOSE Samples in the MINERVE Reactor R1-UO2, R2-UO2, and R1-MOX Configurations, Argonne National Laboratory Technical Report, ANL-GEN-IV-085, September 2006.

4. E.A. Schaefer and J.O. Hibbits, Determination of Oxygen-to-Uranium Ratios in Hypo- and Hyper-stoichiometric Unanium Dioxide and Tungsten-Uranium Dioxide, *Analytical Chemistry*, **41**, pp. 254-259 (1969).

5. A. Gandini, Uncertainty Analysis, Y. Ronen Editor, CRC Press 1988.

6. E. Greenspan, Advances in Nuclear Science and Technology, Vol. **14**, J. Lewins and A. Becker Editors, Plenum Publishing Corporation, 1982.

7. A. Gandini, G. Palmiotti and M. Salvatores, Equivalent Generalized Perturbation Theory, Ann. Nucl. Energy, Vol. **13**, n.3, pp. 109-114, 1986

8. G. Palmiotti and M. Salvatores, Use of Integral Experiments in the Assessment of Large Liquid-Metal Fast Breeder Reactor Basic Design Parameters. *Nucl. Sci. Eng*. **87**, 333 (1984).

9. M. Salvatores, G. Aliberti, G. Palmiotti, D. Rochman, P. Oblozinsky, M. Hermann, P. Talou, T. Kawano, L. Leal, A. Koning, I. Kodeli, Nuclear Data Needs for Advanced Reactor Systems. A NEA Nuclear Science Committee Initiative, ND2007, Nice (France), April 2007.

10. G. Rimpault, et al., The ERANOS Code and Data System for Fast Reactor Neutronic Analyses, Proceedings of PHYSOR 2002 Conference (Seoul, South Korea, October 2002).

11. G. Palmiotti, J.M. Rieunier, C. Gho, M. Salvatores, BISTRO Optimized Two Dimensional Sn Transport Code, *Nucl. Sc. Eng*. **104**, 26 (1990).

12. G. Rimpault, Algorithmic Features of the ECCO Cell Code for Treating Heterogeneous Fast Reactor Assemblies, International Topical Meeting on Reactor Physics and Computation, Portland - Oregon, May 1-5, 1995.

13. JEF3.1, CEA Private Comunication.

14. G. Aliberti and R. Klann, OSMOSE Experiment Representativity Studies, Argonne National Laboratory Technical Report, ANL-AFCI-206, September 27, 2007.

Nuclear Engineering Division
Argonne National Laboratory
9700 South Cass Avenue, Bldg. 308
Argonne, IL 60439-4842

www.anl.gov

UChicago ▶ Argonne LLC

A U.S. Department of Energy laboratory
managed by UChicago Argonne, LLC